ESPOO 2005 VTT PUBLICATIONS 583

Erja Turunen

Diagnostic tools for HVOF process optimization

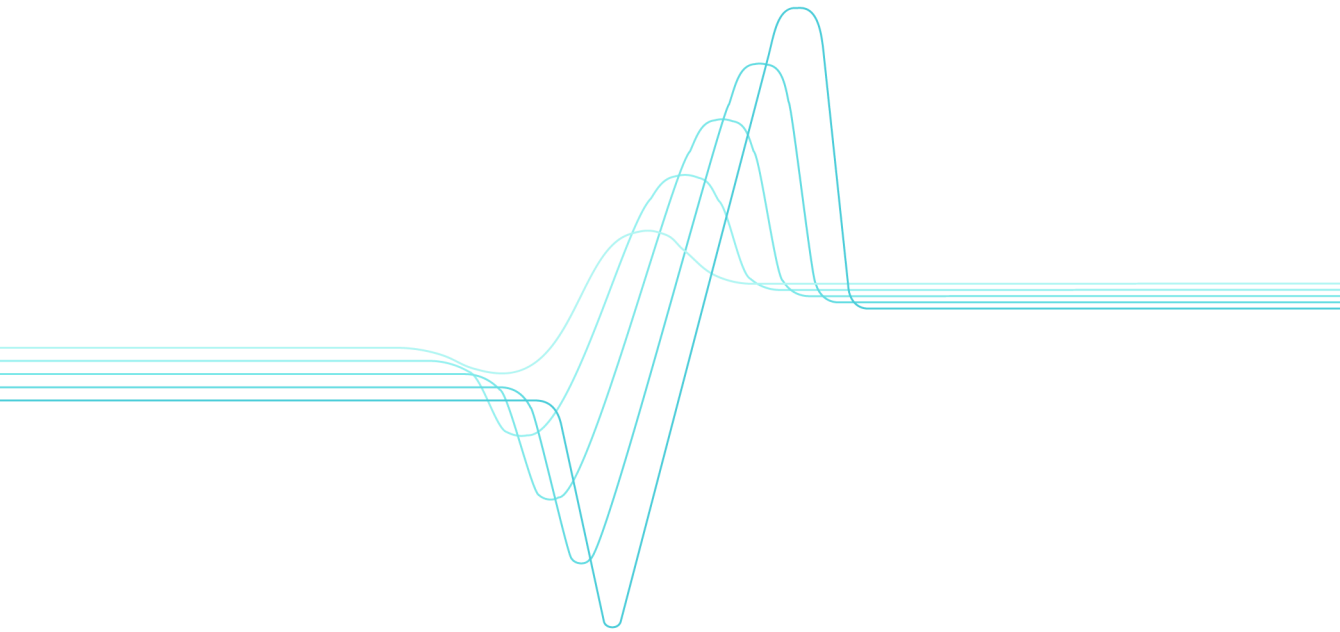

VTT PUBLICATIONS 583

Diagnostic tools for HVOF process optimization

Erja Turunen

VTT Industrial Systems

Dissertation for the degree of Doctor of Science in Technology to be presented with due permission of the Department of Materials Science and Engineering, for public examination and debate in Auditorium 1 (Vuorimiehentie 2 A) at Helsinki University of Technology, Espoo, Finland) on the 16th of December, 2005, at 12 noon.

ISBN 951–38–6677–7 (soft back ed.)
ISSN 1235–0621 (soft back ed.)

ISBN 951–38–6678–5 (URL: http://www.vtt.fi/inf/pdf/)
ISSN 1455–0849 (URL: http://www.vtt.fi/inf/pdf/)

JULKAISIJA – UTGIVARE – PUBLISHER

VTT, Vuorimiehentie 5, PL 2000, 02044 VTT
puh. vaihde 020 722 111, faksi 020 722 4374

VTT, Bergsmansvägen 5, PB 2000, 02044 VTT
tel. växel 020 722 111, fax 020 722 4374

VTT Technical Research Centre of Finland, Vuorimiehentie 5, P.O.Box 2000, FI–02044 VTT, Finland
phone internat. +358 20 722 111, fax +358 20 722 4374

VTT Tuotteet ja tuotanto, Metallimiehenkuja 8, PL 1703, 02044 VTT
puh. vaihde 020 722 111, faksi 020 722 7069

VTT Industriella System, Metallmansgränden 8, PB 1703, 02044 VTT
tel. växel 020 722 111, fax 020 722 7069

VTT Industrial Systems, Metallimiehenkuja 8, P.O.Box 1703, FI–02044 VTT, Finland
phone internat. +358 20 722 111, fax +358 20 722 7069

Otamedia Oy, Espoo 2005

Turunen, Erja. Diagnostic tools for HVOF process optimization. Espoo 2005. VTT Publications 583. 66 p. + app. 92 p.

Keywords thermal spraying, HVOF, high velocity oxi-fuels, process optimizatic diagnostics, single splat studies, surface coatings, alumina, quasicrystals, nanofractions

Abstract

In the thermal spray process the coating is built up from lamellas formed by rapid solidification of the melted or semi-melted droplets attached to the substrate. A typical structure for the coating is a pancake-like lamellar structure, where the flattening stage and adhesion between the lamellas, together with the coating material itself, define the main properties of the coating. Thermal spray coatings are often applied for better corrosion and wear resistance. Therefore, low porosity and good adhesion are desired properties for the coating. High velocity processes – especially HVOF (High velocity oxy-fuel) spraying – are the most potential methods for producing a good adherent coating with low porosity.

From a scientific point of view, particle velocity and particle temperature, together with substrate temperature, are the main parameters affecting the deposit formation. They determine the deposit build-up process and deposit properties. Particle velocity and temperature affect the deposit efficiency as well as the microstructure.

The aim of this work was to show the workability of diagnostic tools in the HVOF process. The focus was on first order process mapping, including on-line diagnostics and single splat studies. Nanocrystalline alumina composites and quasicrystals were selected, two materials that are complex to spray. With both materials the melting state of the particles must be well optimized in order to produce dense, well-adhered coating without unwanted changes in coating phase structure.

The main focus was on the HVOF spraying of alumina. The target was to obtain a systematic understanding of the influence of the process conditions on the

microstructure development in HVOF alumina coatings. Conventional limits of gas ratios and flows were exceeded to obtain a wide velocity-temperature range. The study aimed to produce information for a first order process map, and was carried out at a much deeper level than previously reported. Propylene and hydrogen as fuel gases were compared, and other variables, such as total gas flow rate, fuel gas/oxygen ratio, and standoff distance were also varied. The obtained data was applied for nanostructured alumina composite coatings, and the effect of the process conditions was compared on the obtained coating microstructure and properties.

On-line diagnostic measurements, in which particle temperatures and velocities in the flame can be measured, were performed. The main work was carried out for alumina by using a DPV-2000 system. Two clear regions of different temperature and velocity arise from the use of different fuel gases. Single splat studies correlated well with the obtained coating properties, and a first order process map for alumina was created showing the window for the spray parameters producing best coating quality plotted against coating hardness and abrasive wear resistance.

It was shown that diagnostic results can be correlated with the coating microstructure and coating properties in HVOF spraying. It was also demonstrated that the coating properties and coating quality can be improved by optimizing and carefully selecting the spray parameters.

Preface

The research work for this thesis was carried out in the Surface Engineering group at VTT, the Technical Research Center of Finland, from 2000 to 2005. The work related to Publication IV was partly carried out during the 6 weeks research period I spent at Stony Brook University, USA, in the summer of 2002. The work was then continued in Finland, as well as finalizing the publication. The thesis was supervised by Professor Simo-Pekka Hannula, to whom I would like to express my sincere gratitude for his guidance, support and fruitful discussions around the issues related to this thesis.

My sincere thanks also go to my co-workers at VTT. My closest co-workers, Tommi Varis, Kimmo Ruusuvuori and Maria Oksa, have all been very supportive and understanding during my most hectic period when I was preparing this work. Markku Lindberg, Alpo Viitanen and Seija Kivi get special thanks for their technical support in making coatings and samples. Jari Keskinen, Pertti Lintunen, Teppo Fält and Tom E. Gustafsson have also all an unique role in this co-operation. I also want to thank my group leader, Jari Koskinen, for all his support and late evening discussions, which increased my motivation even more. I want to give special thanks to all the other members of my group for creating such a good and motivating atmosphere to work in.

Acknowledgement is also due to Professor Sanjay Sampath and his group at Stony Brook University, USA, for their co-operation and the resources made available to me. Special greetings go to Jonathan Gutleber and Anirudha Vaidya for those long hours in the spray booth together.

The financial support provided by VTT, the National Technology Agency (Tekes), and Finnish industry is gratefully acknowledged.

I also want to thank my family and friends for all their support, encouragement and care over these years. And, last but not least, I thank Elina for her positive attitude and patience towards my work.

Espoo, November 2005

Erja Turunen

Contents

Appendix I of this publication is not included in the PDF version.
Please order the printed version to get the complete publication
(http://www.vtt.fi/inf/pdf/)

List of included publications

This thesis consists of a summary of the main results and six appended publications I–VI.

I Turunen, E., Varis, T., Vierimaa, K. & Hannula, S.-P. Spray parameter optimisation and tribilogical properties of thermally sprayed quasicrystalline and partially quasicrystalline coatings. Proc. Estonian Acad. Sci. Eng., 9, 4 (2003), pp. 293–303.

II Huttunen-Saarivirta, E., Turunen, E. & Kallio, M. Microstructural Characterisation of Thermally Sprayed Quasicrystalline Al-Co-Fe-Cr Coatings. Journal of Alloys and Compounds, 354, 1–2 (2003), pp. 269–280.

III Huttunen-Saarivirta, E., Turunen, E. & Kallio, M. Influence of Cr Alloying on the Microstructure of Thermally Sprayed Quasicrystalline Al-Cu-Fe Coatings. Intermetallics 11 (2003), pp. 879–891.

IV Turunen, E., Varis, T., Hannula, S.-P., Vaidya, A., Kulkarni, A., Gutleber, J., Sampath, S. & Herman, H. On the role of particle state and deposition procedure on mechanical, tribological and dielectric response of high velocity oxy-fuel sprayed alumina coatings. Materials Science and Engineering. Accepted for publication, in print (2005).

V Turunen, E., Varis, T., Gustafsson, T.E., Keskinen, J., Fält, T. & Hannula, S.-P. Parameter optimization of HVOF sprayed nanostructured alumina and alumina-nickel composite coatings. Surface and Coatings Technology. Accepted for publication, in print (2005).

VI Turunen, E., Varis, T. Gustafsson, T. E., Keskinen, J., Lintunen, P., Fält, T. & Hannula, S.-P. Process optimization and performance of nanoreinforced HVOF-sprayed ceramic coatings. Proceedings of 16th International Plansee Seminar, May 30–June 3, 2005, Reutte, Austria. Pp. 422–433.

Author's contribution

I was the main author of the Publications I, IV–VI. I prepared the test matrixes and schedules, participated in the spray and diagnostic tests, studied the diagnostic data and compared them with the splat results and coating performance data. Co-authors were essential in the following tasks: T. Varis was in charge of the thermal spray studies at VTT, and J. Gutleber and A. Vaidya at Stony Brook University, USA; T. E. Gustafsson made the SEM studies and T. Fält the nanoindentation studies; J. Keskinen produced special nanostructured ceramic powders; and Professor Hannula supervised this work.

E. Saarivirta-Huttunen made separated, wide microscopy studies for quasicrystalline coatings and was the main author of Publications II and III. For those publications, E.T was in charge of thermal spray coating manufacturing, process optimization and coating properties characterization, including microstructure and Pin-on-Disc testing. The button test was carried out by K. Vierimaa of Metso Corp.

List of symbols

HVOF	High velocity oxy-fuel
APS	Atmospheric plasma spray
CTE	Coefficient of thermal expansion
XRD	X-ray diffraction
SW	SprayWatch on-line diagnostic equipment
CCD	Charge-coupled device
IR	infrared
α, γ	Symbols for different alumina phases
SEM	Scanning electron microscope
TEM	Transmission electron microscope
C_3H_6	Propylene
O_2	Oxygen
H_2	Hydrogen
CoF	Coefficient of friction
PoD	Pin-on-disc
QC	Quasicrystal
m/s	meters per second
kW	kilowatts
°C	Celsius degree
kg/h	kilograms per hour
µm	micrometer
nm	nanometer
l/min	litres per minute
∅	diameter

1. Introduction

1.1 Thermal spraying

Thermal spraying is a general term to describe all methods in which the coating is formed from melted or semi-melted droplets. In thermal spraying the material is in the form of powder, wire or rod and is fed into the flame produced by a spray gun, where it melts and the formed droplets are accelerated towards the substrate to be coated. The thermal and kinetic energy of the flame can be produced either with burning mixtures of fuel gas and oxygen, or by using an electrical power source. Based on the energy source, thermal spray methods can be divided into a few main groups: plasma spray methods, flame spray methods, high velocity oxy-fuel methods, electrical arc methods, and, as the latest technology, cold gas methods.[1, 2, 3]

In thermal spraying the coating is built up from the lamellas formed by rapid solidification of the melted or semi-melted droplets attached to the substrate. A typical structure for the coating is a pancake-like lamellar structure, where the flattening degree and adhesion between the lamellas, together with the coating material itself, define the main properties of the coating. The adhesion and porosity of the coating is mainly defined by the particle melting behavior and the velocity when attaching to the surface. In addition, due to the fast cooling rate of the particles, some special features, such as residual stresses and the metastable phases can be observed in the thermally sprayed coatings.[1, 2, 3]

Thermal spray coatings are often applied for better corrosion and wear resistance. Therefore, low porosity and good adhesion are desired properties for the coating. High velocity processes – especially HVOF (High velocity oxy-fuel) spraying – are the most potential methods for producing a good adherent coating with low porosity. In HVOF spraying heat is produced by burning mixtures of oxygen and fuel gas, mainly hydrogen, kerosene, propane, propylene, natural gas or acetylene. Due to the special nozzle design, a jet with supersonic speed is produced. Another commonly used method is APS (Atmospheric plasma spray), where the energy is based on the plasma produced by ionizing an inert gas, typically a mixture of argon and hydrogen or helium, between the anode and the cathode in the spray gun. Due to the high energetic ionized plasma, the temperature of the plasma flame is very high.

The main difference between HVOF and APS is the relationship between the kinetic and thermal energy of the process described by the particle velocity and the flame temperature. Typical ranges of these parameters for each of the process are given in Table 1.

Table 1. Characteristic features of HVOF and APS processes.[3]

Spraying method	**Particle velocity (m/s)**	**Flame temperature (°C)**
HVOF	500–700	~ 3 000
APS	150–400	~8000–12000

The ability to produce dense coatings with low amount of phase transformations and oxidation is the main feature of the HVOF process. This is due to the short dwell time of the particles in a relatively cold flame. It is widely used to produce cermet and metal coatings. The HVOF process has also demonstrated an ability to deposit dense ceramic coatings, such as alumina.[4, 5, 6, 7]

Due to the high process temperature, APS which enables good melting of the ceramic particles is often used to produce a ceramic coating.

The use of thermal spray coatings has traditionally been based on extending the life of the component. However, thermal spray coatings have increasingly been considered "prime reliant" and such coatings are already being included in the design of the systems.[8] This requires considerable enhancement of the reliability and reproducibility of the coatings. Thermal spraying is a very complex process and includes number of variables. A better understanding of the relationship of these variables and their effect on the coating properties must be obtained in order to apply thermal spray coating to "prime reliant" applications.

1.1.1 HVOF Spraying

In the HVOF process the combustion fuel and oxygen are led to the combustion chamber together with the spray powder. The combustion of the gases produces

a high temperature and high pressure in the chamber, which causes the supersonic flow of the gases through the nozzle. The powder particles melt because of the flame temperature in the combustion chamber and during the flight through the nozzle. The flame temperature varies in the range of 2500 °C–3200 °C, depending on the fuel, the fuel gas/oxygen ratio and the gas pressure. In the HVOF process the particles melt completely or only partially, depending on the flame temperature and material's melting point. The degree of melting depends on the flame temperature and the dwell time in which the particles occupy the flame. These are adjustable process parameters and they affect the properties of the coating.[1]

The interest in the HVOF process to produce coatings with a wider range of materials has been growing continuously. For those materials that are sensitive to phase transformations due to evaporation or oxidation, HVOF spray is a very potential coating method due to the process condition, which combines a relatively low flame temperature with a low exposure time in the flame.

A few different HVOF spray systems exist with partly different gun designs and capacities. Each one has differences in design, but all are based on the same fundamental principles. The combination of high pressure (over 4 bar) and gas flow rates of several hundred liters per minute generate hypersonic gas velocities.[7] These systems can be roughly divided into the first, second and third generation. In all first and second generation guns the pressurized burning of gaseous fuel with oxygen is used to produce an exhaust jet traveling at a speed of about 1800 to 2000 m/s. Spray systems belonging to this category are Jet Kote, Diamond Jet (DJ), HV-2000 and CDS. Under standard spray conditions the systems are operated at a power level of about 80 kW and are capable of spraying about 2–3 kg/h of WC-Co. The third generation systems are for power levels ranging from 100 to 200 kW, being capable of spray rates up to about 10 kg/h. The difference between the third generation systems (JP-5000 and DJ Hybrid) and the previous ones is the operation at higher gas/fuel flows and higher chamber pressures (8 to 12 bar versus to 3 to 5 bar). [7, 9, 10]

A comparison of different spray systems has shown that only one model from the second generation can transfer enough heat to the particle to be able to melt a ceramic particle. This system is called Top Gun or HV-2000.[9]

Despite the fact that the first HVOF method was introduced in 1982, there has only been limited effort towards understanding the effect of process parameters on the structure and properties of the coating compared to the work carried out in the field of plasma spraying. The main reason for this is the common use of the method to produce coatings from a few standard materials, such as cermets, where the process parameters are optimized and specified by the powder and equipment manufacturers. In these applications, coating quality optimization is widely carried out form the powder development point of view. Recently, more interest in understanding the HVOF process and the effect of process variables on the coating quality has arisen due to the growing interest in the development of closed loop process control.[10]

1.1.2 Microstructure of thermal spray coatings

The microstructure of a thermal spray coating is a complex mixture of lamellas formed from melted or semi-melted particles as well as many irregularities. Metallic coatings typically contain oxide films due to the oxidation of the particles in the hot flame. Ceramic coatings often contain cracks due to the relaxation of stresses.[11] Three typical groups of porosity can be identified: interlamellar pores, globular pores, and intrasplat cracks.[4] The differences between the pore structures are mainly due to the melting stage and the impact velocity of the particles.[5] Interlamellar pores are parallel to the coated substrate and are typically formed by a reduced cohesion between two splats. Globular pores are formed by the incomplete melting or fast re-solidification of the particles. Intrasplat cracks are perpendicular to the splat interface and are formed by the stress relaxation during cooling of the coating-substrate system with a difference in CTE (coefficient of thermal expansion).[11]

A large number of studies are being carried out to try to understand relationship between the plasma spray process and the coating properties.[12] Only recently have more detailed studies been carried out to try to understand the effect of the HVOF process variables on the coating microstructure and performance more deeply (more details in Chapter 1.2.3).

1.2 Tools for process optimization

From a scientific point of view, particle velocity and particle temperature together with substrate temperature are the main parameters affecting the deposit formation. They determine the deposit build-up process and deposit properties. Particle velocity and temperature affect the deposit efficiency as well as the microstructure.

Different tools are being developed in order to better understand the deposit formation and relationship to the coating properties. These tools are currently being collected under a concept of "Process Map". This can be considered to have two different meanings, aiming at either a) optimization and mapping of the different in-flight process conditions of the particles, producing a different melting range of the particles, or b) finding the influence of different splat structures and substrates on the final structure and properties of the deposited coating. These two maps have lately been named "First order map" and "Second order map" by Prof. Sampath.[8] Figure 1 illustrated the philosophy of such a map.

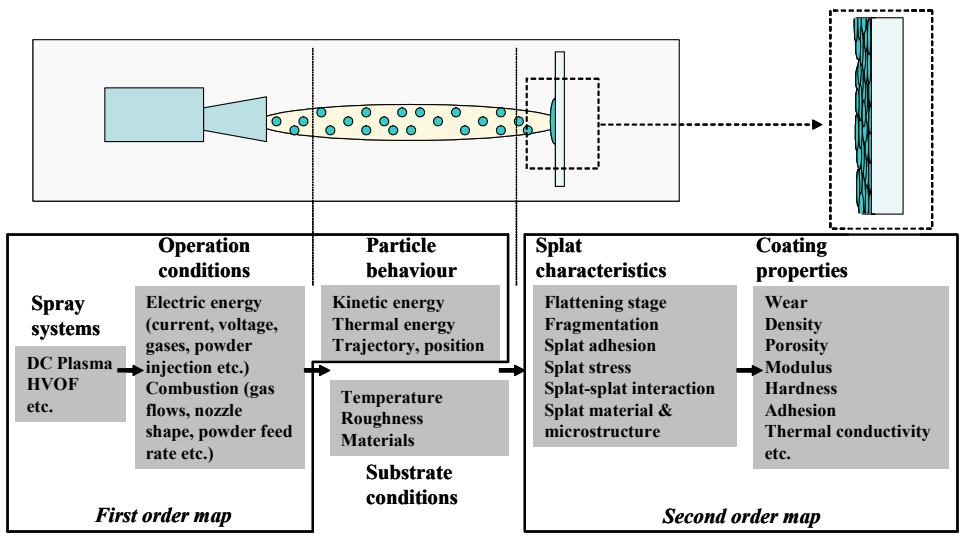

Figure 1. Schematic overview of process maps (modified from reference 8).

Single tools mainly used in process mapping are i) in-flight diagnostics, where particle velocity and temperature are measured during their flight in the flame, ii) splat studies, where the particle melting stage and droplet spreading/solidification is

studied from the behavior of single particles, and iii) droplet/surface or previously deposited layer interaction, where the substrate temperature has been found to have significant influence on the particle morphology, deposit microstructure and properties.[8]

Process maps can also mean equipment and material-specific studies to define the interaction of a certain velocity-temperature range with the final properties of the coating. In this case both diagnostic measurements and mathematical modeling are used to create "a process window" to ensure the desired coating microstructure within certain approved limits of parameter fluctuations.[13]

On-line diagnostic and single splat diagnostic tools are presented in more detail in Chapters 1.2.1 and 1.2.2. The effect of HVOF process variables on the coating microstructure and properties is discussed in more detail in chapter 1.2.3.

1.2.1 On-line diagnostic methods

Different on-line diagnostic tools have been developed to be able to measure direct thermal spray jet properties such as enthalpy, particle temperature, particle velocity, particle size and total particle flux. These are the main parameters that influence the characteristics of the deposited coating. On-line diagnostic tools can be used either for process optimization of thermal spray coating with certain material and spray processes or for process control during deposition.

The most sophisticated systems are too complex for process control. Therefore, a large number of simple, fast, and cost effective systems for the measurement of the jet shape and direction, ignoring information on single particles, have been developed, such as Particle Flux Imaging-PFI, DifRex M, PlumeSpector and SDC.[14]

The enthalpy available in the jet can be measured by using enthalpy probes specially developed for the measurement of enthalpy, temperature and velocity of gaseous effluents. This technology gives overall information on the jet properties, but, depending on the spray material, no detailed information on the particle conditions or other spray conditions, such as gas pressure.[15]

More sophisticated tools are needed when more detailed information on a single particle is wanted, as is the case in process optimization work. The most advanced on-line diagnostic tools are based on the measurement of the thermal emission of the particles. In these systems the temperature is determined using a two-color pyrometer and velocity determined from images captured with fast CCD camera systems.[16] Single particle techniques require that the number of particles is limited in some methods due to the ability to observe the light emitted by a single particle without overwhelming interference from surrounding particles. Depending on the technology, the amount of powder varies from a few tens of grams to the normal powder feed rate up to 5–10 kg/h. This limits the usability of some technologies in quality control applications in real production work.

Only a few commercial equipment applications are suitable when detailed information on particles is wanted for different spray conditions in order to optimize spray parameters. This is especially the case in HVOF spraying, where particle velocities are high and particle temperatures are low compared with the plasma spray.

Temperature measurement is based on the optical system and on the well-known fact that objects emit electromagnetic radiation, in which the intensity and wavelength depend on the temperature of the object; the radiation is shifted towards shorter wavelengths during heating. Measurement is based on the two-color pyrometer measuring the radiance of hot, incandescent particles. Two-color pyrometer is a method for optical temperature measurement that is based on the measurements of the light emitted by the object in two separate wavelength ranges. The method eliminates the effect of particle size, emissivity and non-ideal focusing, and is, therefore, usable with all materials without material specified calibration[17]. For lack of better information, the particles are generally assumed to behave as gray body emitters[18]. This will cause some inaccuracy in the measurements, especially in the case of metal particles where the error can be up to 100 °C[17].

The measurement of particle velocity is generally performed by laser Doppler velocimetry or by transit timing techniques.[18]

DPV-2000 (Tecnal Ltd) is based on two-color pyrometry at two different spectral ranges in the near IR wavelength region around 790 nm and 990 nm,

respectively. The particle velocity is determined by the on-flight technique during the passage of particles in front of a two-slit mask.[19] The mean and standard deviation of the particle temperature distribution can be obtained from observations of sufficient numbers of individual particles.[20] The measurement spot is small and the positioning must be performed carefully. The measurement is also relatively insensitive to spatial movement of the spray pattern. If information through the whole flame is required, the measurement must be performed by scanning the probe, which increases the measurement time for several minutes per condition. The benefit of the system is in its ability to measure dimensional information on single particles.

SprayWatch (Oseir Oy) is based on the CCD camera. The particles are imaged onto a CCD camera sensor with the aid of spectrally resolving optics. Particle velocity is measured using the time-of-flight method. The length of the particle traces on the CCD detector is measured by the image processing algorithm, and is then converted to velocity by dividing it by the known camera shutter time[17, 21]. The temperature of the particles is measured with two-color pyrometry. The benefit of this technique is the possibility to obtain information through the whole jet. A disadvantage is that the information is always an average, and, therefore, the temperature values are lower than the values obtained by DPV-2000 when measured from the centre of the jet.

It is shown that particle velocity and temperature varies widely at different positions in the jet, and monitoring of particle properties at one single position in the jet is not sufficient for describing the complete particle jet.[22]

1.2.2 Splat studies

Splat forming research studies have been carried out to better understand the relationship between the particle in-flight conditions and the coating microstructure. The bulk of the work has been done in the field of plasma spraying and some important results have been produced. The research work has been carried out by both theoretical simulations and experimental observations.

The splat morphology is described with various terms, including mushroom-like, pancake-like, flower-like, and fingered-like splats[23, 24]. Splat morphology has

important implications for the coating microstructure development, porosity and, finally, coating properties. It can be concluded that the main factors affecting the splat morphology are particle velocity, particle temperature, substrate temperature and the Reynolds number of the particle[24, 25]. Many other parameters, such as impact angle, particle surface chemistry, and many substrate parameters, including contamination by condensates and absorbates, oxidation stage, roughness and thermal properties, also have an effect[25].

Fukanuma et al.[26] have classified the formation of splat into four different groups: 1) the molten viscous particle impinges and spreads as a thin disc, 2) the molten viscous particle impinges and splashes with some part of the particle remaining on the substrate, 3) the plastic particle impinges and is deformed plastically, 4) the elastic particle impinges and bounces off the substrate. The first two are the main mechanisms for thermal spray coating formation, including particle melting. Fukanuma's classification does not consider the cases when particles are only partly melted or when the spray material does not deform plastically.

More detailed studies are being carried out on the complete molten droplets. It has been found that no significant solidification of the splat occurs before the spreading is complete. The spreading of the liquid stops when the kinetic energy of the droplet is dissipated[23]. Temperature has been recognized to have an important role both in the splat morphology and the splat dimension forming. An increase in the substrate temperature will produce a more uniform splat with a lower amount of fragmentation. The phenomenon has been shown to occur at relatively low substrate temperatures for most materials (100–400 °C).[27] An increase in the Reynolds number has shown a trend for an increased cooling rate in the lamella.[28] An increase in particle temperature has also been shown to have an effect on the splat morphology: an increased particle temperature lowered the droplet viscosity, and the fragmentation of the alumina particle was increased[24].

All the studied particle conditions have particle velocities of less than 50 m/s, and thus the findings in these studies cannot be directly used in the case of high velocity spraying where particle velocities are hundreds of meters/second.

Splat formation for high velocity spray methods has not been studied in such detail. The previous work has mainly concentrated on a demonstration of

different molten stages of the particles in different spray conditions and on the effect of that for the coating microstructure and properties[4, 29, 30, 31, 32]. Sobolev et al. have developed a uniform model to estimate the flattening of the composite powder that is also suitable for HVOF spraying[33, 34]. Work within high velocity spraying is mainly being carried out for metal and hardmetal coatings. Only Kulkarni[4] and Sundararajan[29] have published some splat studies for high velocity spraying of alumina.

1.2.3 HVOF process optimization

So far, only a small amount of work has been carried out in order to understand the different phenomena behind HVOF spraying.

The creation of a first order process map in the case of HVOF would include interaction studies between spray parameters, such as fuel gas/oxygen ratio, total gas flow and standoff distance on the velocity-temperature behavior of the particle and the splat structure. A second order map would include a coating properties evaluation, such as residual stresses, porosity, adhesion, hardness, mechanical properties, and wear/corrosion resistance compared with the different splat structures.

Some comparison between different spray processes – mainly APS and HVOF – has been carried out. The differences in particle velocity and temperature between these two processes, and their effect on the properties of metallic coating, have been clearly demonstrated by Sampath et al.[35]

A more detailed study on the effect of different fuel gases in HVOF spraying has been carried out by Lugscheider et al.[36] They investigated MCrAlY powders and noticed that higher flame temperatures are obtained by using propane compared with hydrogen as a fuel gas. An increase in standoff increased particle temperatures. Particle velocities were higher when spraying with hydrogen. The findings were screened towards the oxygen content and oxidation resistance of the MCrAlY coatings. Similar results were obtained by Lugscheider et al.[31] and Hanson et al.[37] for AISI316L stainless steel.

Planche et al.[38] have studied the influence of the HVOF spray parameters on the in-flight characteristics of Inconel 718 particles and their correlation with the electrochemical behavior of the coating. In their studies the total gas flow was not constant between different spray conditions, so it is not possible to directly compare their results with the other published results. However, in their measurements particle velocity increased with an increasing total gas flow rate and the temperature was highest at fuel-rich conditions.

The relationship between different HVOF spray parameters for NiWCrBSi coatings and the corrosion performance of the coatings was studied by Gil et al.[39]. They varied a number of parameters and found that only standoff distance, fuel gas/oxygen and powder feed rate formed a clear correlation for porosity and corrosion resistance.

Li et al.[10, 40, 41] have recently carried out extensive research aiming to understand the relationship between gas parameters and particle temperature and velocity in the flame. Their main target is the development of model-based estimations of particle velocity and temperature aiming at the design of closed loop process control for the HVOF spray system[10, 40]. The first part of the modeling work concentrated on modeling the gas phase and particle behavior[41]. The latter part of the large modeling work has been the creation of a rule-based modeling of the coating microstructure. In that model the velocity, temperature and degree of melting of the particles hitting the substrate are determined by a mathematical model.[42] So far, the simulations and modeling are mainly being carried out for nickel with different particle sizes.

Calculations and simulations are also being carried out by other researchers aiming at a better understanding of the HVOF process.[54, 43] Optical flow visualization techniques are being used to examine the rapid turbulent mixing of the supersonic jet with the surrounding atmosphere.[44] However, despite the deep understanding of the gas dynamics, a gap exists in the understanding of the melting behavior of the particle in the jet. Some other studies are also being performed to optimize the process conditions in HVOF spray, but these are mainly focused on the metal or cermet materials and only a few different spray conditions are being measured.[45, 46, 47, 48]

Some results for the optimization of HVOF spraying of ceramics have been published with a limited amount of diagnostic results[49, 50]. Furthermore, investigations have been published for detonation spraying of alumina. The main findings of the studies were that the spray parameters have a strong effect on the coating quality, such as hardness and porosity. The best coating was obtained with a fuel gas/oxygen ratio of 0.28 and with a spray distance of 145 mm[51]. Some work is also being carried out to understand the correlations between spray conditions and microstructure for alumina coatings produced by HVOF and plasma spray. [4, 5, 6, 7, 52, 53] In these studies the coatings are produced using different spray methods, and such coating properties as microstructure, elastic behavior and wear resistance have been compared among the coatings. Other work published for HVOF spraying of alumina mainly focuses on the optimization of deposition parameters via determination of deposition efficiency and coating properties[6, 7]. In some studies the melting capability of different fuel gases has been compared and it has been found that despite the higher flame temperature of the acetylene-oxygen flame, the best coating structure is obtained when using hydrogen[6, 7]. Previous work carried out for a deeper understanding of the HVOF process for ceramics mainly focused on mathematical calculations[5, 54]. It has been shown that sufficient melting of the ceramic particles in the supersonic flame is critical due to the heat energy distribution during the HVOF process; the particles spend most of their time in the supersonic part of the flame, where the temperature is lower compared with the combustion chamber.[54]

Only a few studies concerning thermal spraying of quasicrystalline materials have been published. The studies have mainly focused on APS spraying of quasicrystals, the coating structure thus produced and the behavior of produced coatings in different wear and corrosion tests[55, 56, 57, 58, 59]. Some comparison between APS and HVOF sprayed coatings is presented[60, 61, 62]. These studies have focused on differences in the coating structure and behavior when produced with different thermal spray systems. No process optimization work is presented.

1.3 Coating materials and properties

The crystal structure depends upon the conditions under which the liquid droplets solidify. Due to the rapid cooling of the droplets in the thermal spray process, metastable phases can be produced.

In this study two different coating materials are introduced based on their different requirements for optimal spray conditions.

- Alumina was selected as a representative material that has a high melting point. The target was to spray nanostructured alumina by combining sufficient melting to ensure good lamella adhesion with the capability to retain a nanostructured composite structure.
- Quasicrystal materials were selected due to their sensitivity to composition changes in the flame. The spray parameters for these materials should be optimized in order to produce dense coatings without phase transformations.

1.3.1 Alumina

Ceramic coatings offer an interesting alternative protective layer over a steel structure due to their excellent chemical, corrosion and thermal resistance.[4, 5, 7, 63, 64]. Thermal-sprayed alumina coatings also show interesting electrical properties and can offer an economical solution as dielectric coatings in a variety of thick film and insulated metal substrate-based electronics applications[64, 65]. The melting point of alumina is 2049 °C[66], which is only slightly below the flame temperature produced in the HVOF process. Therefore, from the point of view of HVOF process, it is a challenging material to spray. The HVOF process is of special interest when aiming at dense ceramic layers for environmental protection applications.

A stable phase for alumina at room temperature is hexagonal α-Al_2O_3. Alumina also has a large number of metastable crystalline phases.[67] Due to the rapid cooling during the thermal spray process, these metastable phases are commonly recognized to form in the coating. Process variables in the thermal spray process give a wide spectrum of phase structures. Alumina coatings are reported to mainly consist of α-, γ- and δ-phases[68], of which cubic γ-alumina is the most reported metastable phase.[6, 69] The gamma phase has also been reported to be the dominant phase in the coatings.

The mechanical properties of alpha alumina are better than those of gamma-alumina and this phase is basically more desirable. The physical and electrical

properties are also different[5]. However, the final properties of the coating depend on the coating microstructure, especially on the bonding between the splats.

Plasma spraying of alumina has been studied much more widely than HVOF spraying. Studies have been carried out on the phase structure of the thermal sprayed coatings by using different spray methods, but the results reported are not all in line. Some studies show that the α phase content is lower in the HVOF sprayed coatings compared with the plasma sprayed coatings, suggesting that more complete melting occurs in HVOF spraying due to the differences in powder trajectories and heat transformation[5]. However, most of the studies have shown that the resulting alpha content is somewhat higher when using HVOF spray than the plasma spray.[4, 6, 7]

1.3.2 Nanostructured alumina

Nanocrystalline materials have been recognized as having special mechanical properties. Typically, the strength of crystalline materials increases with decreasing grain size and materials with a small grain size often exhibit superplastic behavior at elevated temperatures. Furthermore, the hardness and wear properties of the coatings are usually improved. There are several recent reviews on the mechanical properties of nanocrystalline materials[70, 71, 72]. Nanocrystallinity has been shown to have a positive influence on the toughness of ceramic materials when alloyed with nanophased metals[73, 74]. The ceramic coating research is mainly focused on development of APS alumina-titania coatings (grain size below 70 nm).[75, 76, 77, 78]

HVOF offers an interesting opportunity to combine dense coatings with a minimum amount of grain growth because of the higher particle velocities when compared to the plasma spray.

1.3.3 Quasicrystals

Quasicrystals are materials in which a repeating periodicity in an atom arrangement exists together with a rotational symmetry forbidden to crystalline materials; fivefold, eightfold, tenfold and even twelvefold symmetries have been encountered in quasicrystals.[79] A large number of properties that are not

common in material based on metal elements have been reported, including high hardness, low coefficient of friction, good oxidation and corrosion resistance, low thermal conductivity and low electrical conductivity.[80]

The majority of studies on thermally sprayed quasicrystalline coatings have concentrated on the different modifications of the ternary base alloys Al-Cu-Fe and Al-Ni-Co[55, 56, 57, 58, 60, 61, 62] by plasma spray.

Sprayed material is sensitive to phase transformations due to the changes in composition during the in-flight phase, such as evaporation of some elements or oxidation. The quasicrystal phase is rather sensitive to the correct elemental composition and can, therefore, be easily transformed from the original quasicrystal structure to the other inter-metallic phases due to the evaporation of some single elements such as alumina or copper during the in-flight phase of the particle in the thermal spray flame. Material stability depends on the spray parameters and the stability of the starting material.[59]

1.4 Aim of the research

In order to produce a coating with the desired properties it is not enough to just control the material structure inside one lamella. The interaction between lamellas, the stress states of the final coating, the adhesion to the substrate and cracking must also be controlled. The different phenomena affecting the final quality of the coating are described schematically in Figure 2.

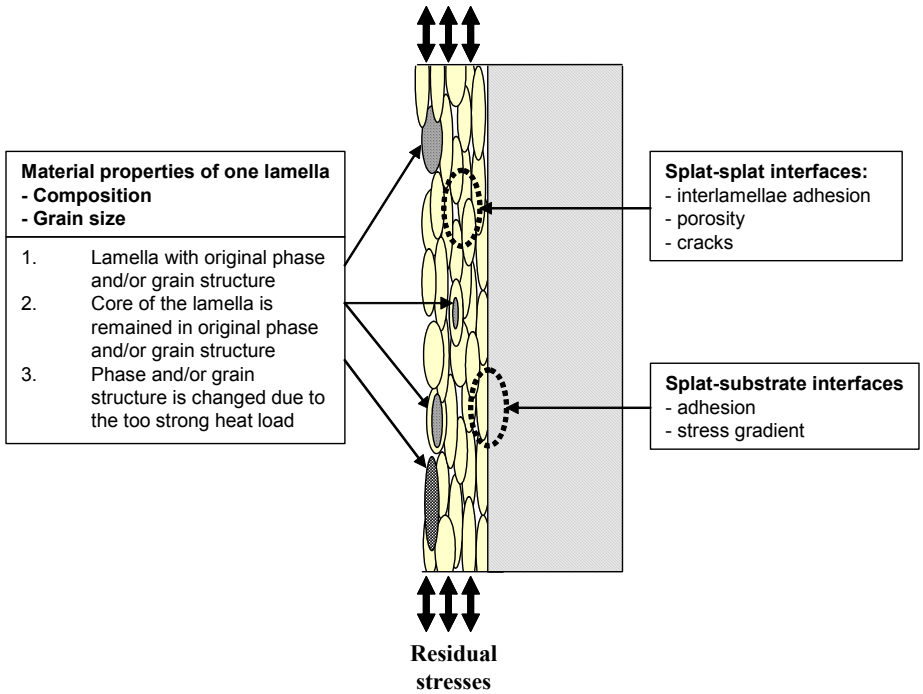

Figure 2. Factors influencing the quality of thermally sprayed coating.

The usability of diagnostic tools, on-line diagnostics and single splat studies is widely demonstrated for plasma spraying. Process mapping as a wider technique is also partly demonstrated for plasma spraying.

The aim of this work was to show the workability of diagnostic tools in the HVOF process. The focus was on first order process mapping, including on-line diagnostics and single splat studies. Nanocrystalline alumina composites and quasicrystal were selected, two materials that are complex to spray. With both

materials the melting state of the particles must be well optimized in order to a produce dense, well-adhered coating without unwanted changes in coating phase structure.

The main focus was on the HVOF spraying of alumina. The target was to obtain a systematic understanding of the influence of the process conditions on the coating microstructure development in HVOF spraying of alumina coatings. Conventional limits of gas ratios and flows were exceeded to obtain a wide velocity-temperature range. The study focused on producing information for a first order process map, and was carried out at a much deeper level than previously reported. Propylene and hydrogen as fuel gases were compared, and other variables, such as total gas flow rate, fuel gas/oxygen ratio, and standoff distance were also varied. The obtained data was applied to the manufacturing of nanostructured alumina composite coatings, and the effect of the process conditions was compared with the obtained coating microstructure and properties.

In the case of quasicrystals, the effect of spray conditions on the formed phase structure of the coating was studied. The main focus was to study whether the evaporation of some critical elements, such as aluminum, can be controlled by varying the spray conditions.

The main focus was placed on the online diagnostic measurements and single splat studies i.e., on the information for a first order process map. Despite the fact that this information was plotted against some coating properties, the creation of full information for a second order process map is not included in this work.

The hyphothesis of this work was that by using diagnostic tools, mainly on-line diagnostics and single splat studies, the formation of the HVOF coating structure can be predicted and the diagnostic tools can be used for process optimization when aiming at a coating with a certain structure and properties.

2. Experimental methods

2.1 Materials

Commercial alumina powder Al-1110HP from Praxair Inc. (39 Old Ridgebury Road, Danbury, CT 06810 USA) was used for the process optimization and as reference powder in the material development work due to the easy availability of the powder. Agglomerated nanofraction alumina powder produced by VTT was used as another reference powder in the process optimization. Synthesis of n-Al_2O_3 powder with and without alloyed nanoparticles was carried out using boehmite (AlO(OH)) as a starting media (trade name Disperal from Sasol Germany GmbH, Anckelmannsplatz 1, 20537 Hamburg, Germany). Nanofraction and nanocomposite powders were manufactured in various ways by using chemical and mechanical routes. The powder preparation has been discussed in Publications V and VI. Table 2 summarizes the sprayed powders.

Table 2. Sprayed alumina powders.

Powder	Material code	Manufacturer and method	Agglomerate size [µm[	Crystal size
Al-1110	ref-Al_2O_3	Praxair, fused and crushed	5–22	conventional
Boehmite	n-Al_2O_3	VTT, agglomerated and sintered	2–25	< 200nm*
Boehmite	n-Al_2O_3 -2% Ni	VTT, agglomerated and sintered	4–23	< 200nm*
Boehmite	n-Al_2O_3 -5% Ni	VTT, agglomerated and sintered	2–26	< 200nm*
Boehmite	n-Al_2O_3 -5% NiO	VTT, agglomerated and sintered	2–21	< 200nm*
Boehmite	n-Al_2O_3 -5% ZrO_2	VTT, agglomerated and sintered	2–29	< 200nm*
Boehmite	n-Al_2O_3 -5% SiC	VTT, agglomerated and sintered	2–29	< 200nm*

*given by the manufacturer

The quasicrystal powders used in this work were manufactured by Saint-Gobain Advanced Ceramics SNMI, France. Details of the used powders are presented in Table 3.

Table 3. Sprayed quasicrystal powders.

Powder	Material	Nominal composition*	Particle size [µm] *	Particle size (measured) [µm]
Christome F1	Al-Cu-Fe	40.8 wt.% Al 41.2 wt.% Cu 17.0 wt.% Fe 0.8 wt.% B	20–53	30–59
Christome A1/S	Al-Cu-Fe-Cr	54.1 wt.% Al 17.8 wt.% Cu 13.0 wt.% Fe 14.9 wt.% Cr	20–53	30–59
Christome BTI	Al-Co-Fe-Cr	52.8 wt.% Al 20.4 wt.% Co 15.3 wt.% Fe 11.2 wt.% Cr.	20–53	23–50

*given by the manufacturer

2.2 Thermal spray test setup

The coatings were deposited using a Praxair HV-2000 spray gun and combustion chambers having lengths of 12mm, 19mm and 22mm. Nitrogen was selected as the carrier gas. The fuel gases were hydrogen and propylene.

2.3 On-line diagnostics

Online diagnostic measurements were carried out using two different types of equipment: Tecnar DVP-2000 and Oseir Spraywatch 2i. The main work was carried out for alumina by using the DPV-2000 diagnostic system. A large number of different spray conditions were measured by varying the total gas flow from 243 l/min to 361 l/min for propylene, and from 893 l/min to 1,050 l/min for hydrogen. Within a certain total gas flow the fuel gas/oxygen ratio was varied from 0.15 to 0.36 for propylene, and from 1.92 to 3.29 for

hydrogen. The stoichiometric ratios are 0.25 for propylene and 2.00 for hydrogen. Other variable parameters were standoff distance, from 150,mm to 200 mm, and length of the combustion chamber, 19 mm and 22 mm. Typically used spray conditions were exceeded in purpose to produce as wide a velocity-temperature range as possible.

For quasicrystals, two spray conditions were measured by changing the standoff distance from 150 mm to 375 mm. The total gas flow in both conditions was 900 l/min and the fuel gas/oxygen ratio was changed, being 2.83 and 2.21.

2.4 Single splat studies

Single splats were collected on polished steel substrates in order to study the melting level of the particles under different spray conditions. The splats were produced by spraying a low powder feed rate using the same standoff distance as was used in the coating deposition.

Splats collected were studied by optical microscopy to determine the extent of melting of the particles. While the temperature data from diagnostic tests, based on the emissivity of a particle in-flight, provide the surface temperature of the particle, single splats enhance our understanding on the particle state.

Despite the fact that splat collection over a polished surface does not give exact information of the splat spreading over a rough surface, it will give important information of the melting state of the particles in different spray conditions. Studying effect of surface roughness of the splat behavior is included for the process map 2, and is therefore excluded from this study. Table 4 summarizes the spray parameters used for splat studies.

Table 4. Spray parameters in splat studies.

alumina					
Ratio C_3H_6/O_2	**Total flow [l/min]**	**Standoff [mm]**	**Ratio H_2/O_2**	**Total flow [l/min]**	**Standoff [mm]**
0.28	361	150	2.00	1.050	150
0.28	361	200	2.48	1.050	150
0.22	361	150	2.85	1.050	150
0.28	283	150	2.85	1.050	200
			2.17	890	150
			2.85	890	150
quasicrystals					
			2.21	900	150
			2.21	900	225
			2.21	900	300
			2.21	900	375
			2.83	900	150
			2.83	900	225
			2.83	900	300
			2.83	900	375

2.5 Coating deposition

The coatings were sprayed onto grit-blasted carbon steel plates. Table 5 summarizes the spray parameters used in the coating experiments.

Table 5. Spray parameters for coatings.

alumina					
Ratio C_3H_6/O_2	**Total flow [l/min]**	**Standoff [mm]**	**Ratio H_2/O_2**	**Total flow [l/min]**	**Standoff [mm]**
0.28	361	150	2.00	1.050	150
0.28	361	200	2.48	1.050	150
0.22	361	150	2.85	1.050	150
0.28	283	150	2.85	1.050	200
			2.17	890	150
quasicrystals					
			2.21	900	300
			2.83	900	300

2.6 Characterization

The crystal structures of the powders and coatings were characterized by X-ray diffraction (XRD) using Cu-K_α and Mo-K_α radiation. Powder particle size was determined using a Lecotrac – LT100 particle size analyzer.

The scanning electron microscopes used in this work were a JEOL JSM-6400 (SEM) combined with a PGT PRISM 2000 X-ray analyzer, a LEO982 Gemini (FEG-SEM), a Philips CM 200 (FEG-STEM) combined with a Noran Voyager X-ray analyzer, a LEO 1550 model with a Schottky Field Emission gun and a Siemens XL30 equipped with an energy dispersive spectrometer model DX-4 by EDAX. The details of the microscopy used in each study are given in publications related to this work.

Free-standing deposits were evaluated for the porosity content using a Helium pycnometry technique. The skeletal density of the coating in this measurement was measured by the volume of gas (Helium) displaced by the known mass of the substance.[81]

The hardness of the coatings was determined by the Vickers microhardness method using a mass of 300 grams. Instrumented nanoindentation tests with Nanotest 550 and Nanotest 600 instruments, both from Micro Materials Limited UK, equipped with a 0.79 mm ball indenter, were used to characterize the elasto-plastic properties of the coating. Calculation of the elastic modulus was made using the method developed by Field and Swain[82].

The wear resistance of the alumina coatings was evaluated by a rubber wheel abrasion test according to the ASTM G 65-91 standard. The coefficient of friction of the quasicrystal coatings was determined using the Pin-on-Disc test method at room temperature and at 500 °C. The test was carried out according to the ASTM 99 standard. A button test was carried out to study the influence of contact pressure and temperature on friction and wear with higher loads. The test is explained in detail in Publication I.

The thermal conductivity measurements were carried out on a 12.5 mm (0.5”) diameter disk, coated with carbon on both surfaces, using a Holometrix laser flash thermal diffusivity instrument. In this test, the sample is irradiated

uniformly on one side using a single laser beam pulse (1.06 μm wavelength). The temperature rise on the other side is recorded as a function of time using an HgCdTe infrared detector (2–5.5 μm wavelengths). The recorded temperature-rise data, with allowance for the measured sample thickness, are used to calculate the thermal diffusivity directly. Knowledge of the bulk density, together with the thermal diffusivity and specific heat, allows determination of the thermal conductivity.[83]

The dielectric properties were measured using an HP 4294A Impedance Analyzer according to ASTM D150. Using parallel plate principles, the dielectric behavior was observed from 40 Hz to 100 MHz; the values at 10 kHz and 1 MHz are reported here.

The electrical strength of the coatings was tested according to IEC 60243-1 C1.9.1 by increasing the voltage up to the breakdown point. A brass electrode, ∅25 mm, was used over the coating, and a larger brass electrode, ∅75 mm, was placed under the specimen. The voltage was increased linearly from zero up to breakdown with a rate of rise 0.03–0.05 kV/s.

3. Results

3.1 Powder characterization

3.1.1 Alumina

Figure 3 shows the typical morphology of the agglomerated composite powder.

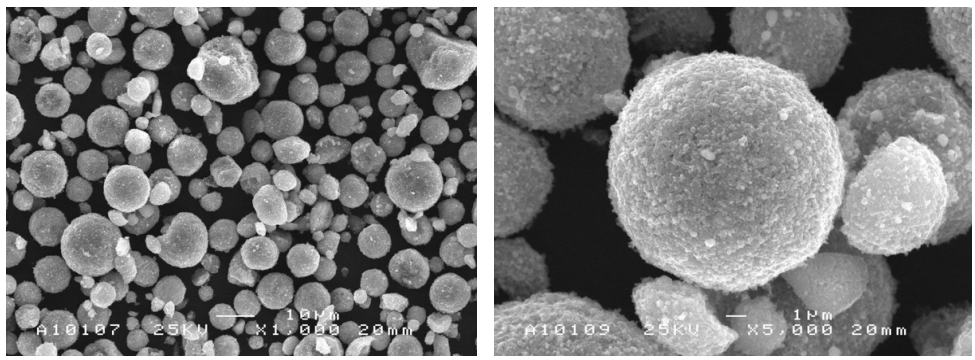

Figure 3. SEM micrographs of the spray-dried Al_2O_3 – 5%Ni particles at a magnification of 500× and 2500×.

3.1.2 Quasicrystals

The quasicrystal powders were analyzed by SEM and Figure 4 shows the morphologies of the quasicrystal powders.

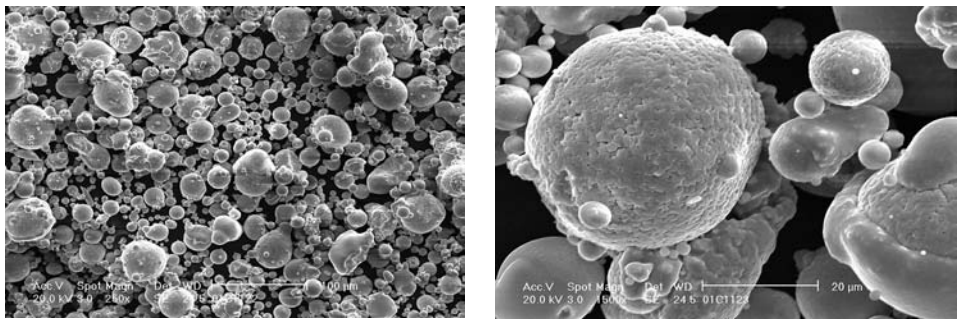

a)

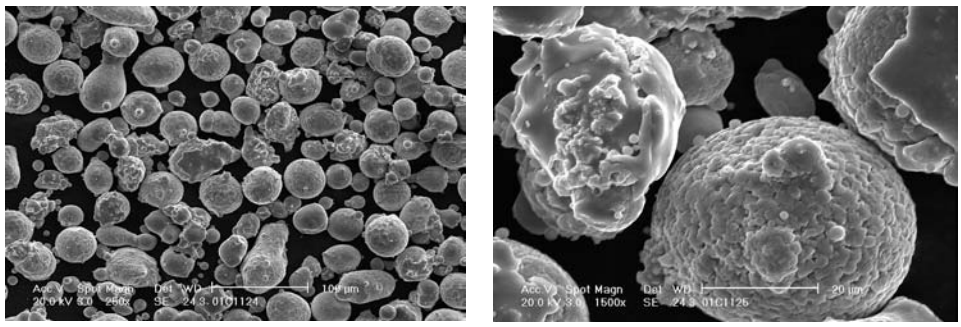

b)

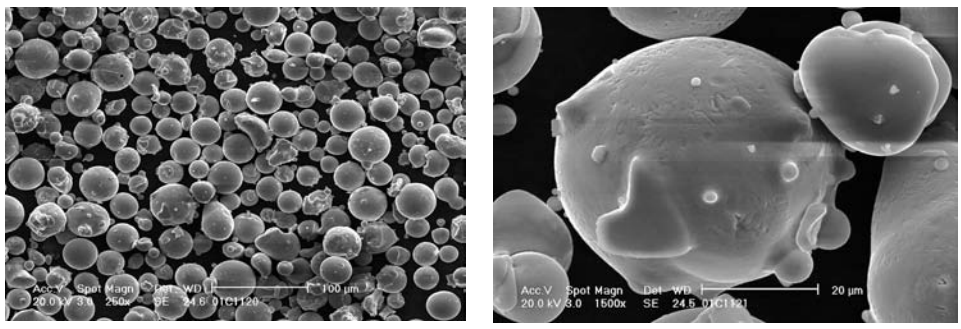

c)

Figure 4. SEM micrographs of the quasicrystal spray particles at a magnification of 125× and 750×. a) F1 powder, b) A1/S powder, c) BTI powder.

3.2 Process optimization

3.2.1 On-line diagnostics

Two different types of on-line diagnostics equipment, DPV-2000 and SprayWatch, were used to determine the effects of variations in the fuel gas, the gas ratios and the total gas flow on the particle velocity and temperature range.

The main work was carried out for alumina by using a DPV-2000 system. Two clear regions of different temperature and velocity arise from the use of different fuel gases as presented in the Figure 5. The operating range of the gas flows and fuel to oxygen ratios was quite different for the two mixtures. The hydrogen-oxygen mixtures typically resulted in a greater velocity of the particles than the propylene-oxygen mixtures. On the other hand, a higher variation between the minimum and maximum values in temperature and velocity was obtained with propylene than with hydrogen. The highest temperatures for propylene were obtained using a fuel gas/oxygen ratio of 0.30. In the case of hydrogen as a fuel gas, the highest temperature was obtained by using a ratio of 2.48.

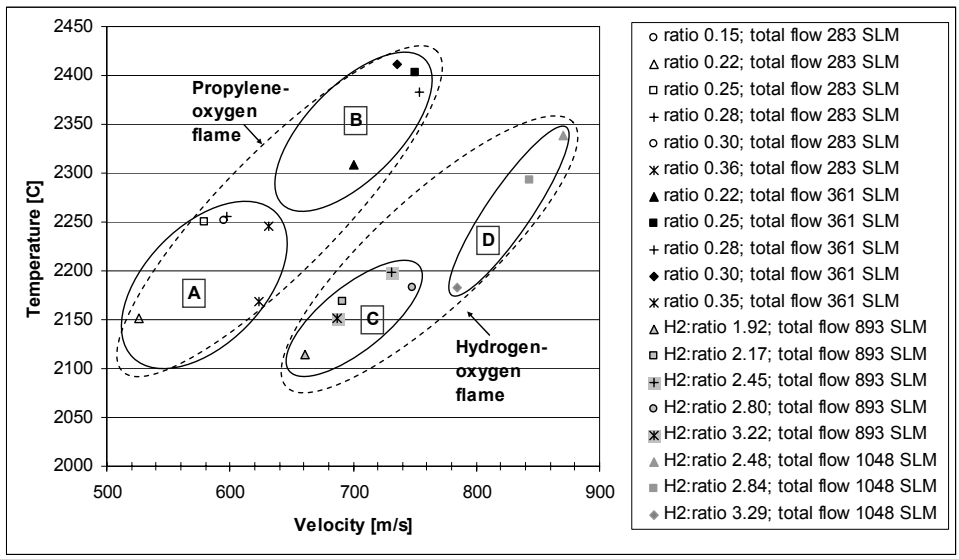

Figure 5. A first order process map for HVOF alumina depicting the range of particle temperatures and velocities for two fuel gas/oxygen mixtures.

Figure 5 also summarizes the findings of the diagnostic study from altering the total gas flow and oxygen/fuel gas ratio. In the Figure, (A) and (B) refer to the zones of velocity and temperature achieved by using a gas mixture of propylene and oxygen while maintaining a total gas flow of 283 l/min and 361 l/min respectively. In general, there was a strong correlation between the velocity and temperature since the two total flow rate zones were separated quite clearly. A similar effect was observed for the zones (C) and (D), which are the values for hydrogen – oxygen gas mixtures with total flow rates of 893 l/min and 1,048 l/min. Within each group of conditions, there is a systematic variation of particle condition depending on the operating parameters.

The total gas throughput flow through the gun had a strong influence on the gas velocity and temperature. Because of this, an almost linear increase in both particle velocity and temperature for a certain fuel gas/oxygen ratio was measured as shown in Figure 6.

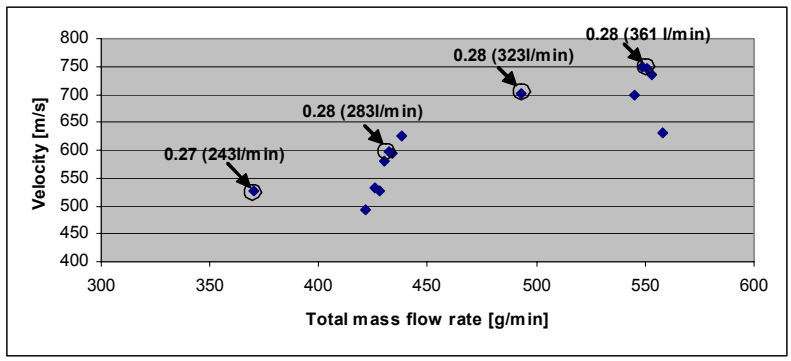

a)

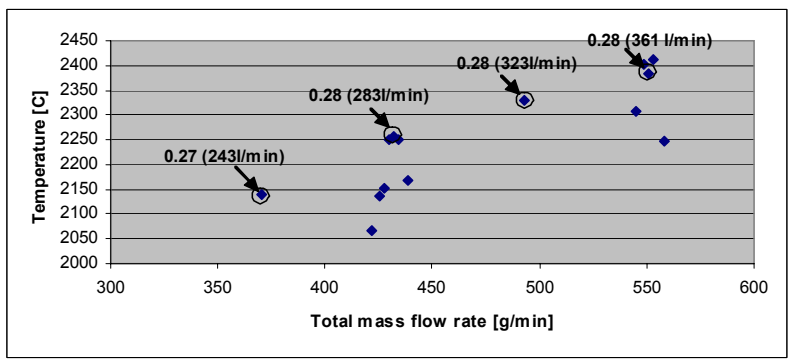

b)

Figure 6. Effect of total gas throughput flow on a) velocity, and b) temperature.

Within a certain total gas flow between different fuel gas/oxygen ratios it was recognized that maximum particle velocities are nearly always obtained at the same time as maximum temperatures. The temperature-velocity maximum was obtained with fuel-rich conditions. Figure 7 shows this trend for the propylene with a total gas flow of 361 l/min, and for hydrogen with a total flow of 893 l/min.

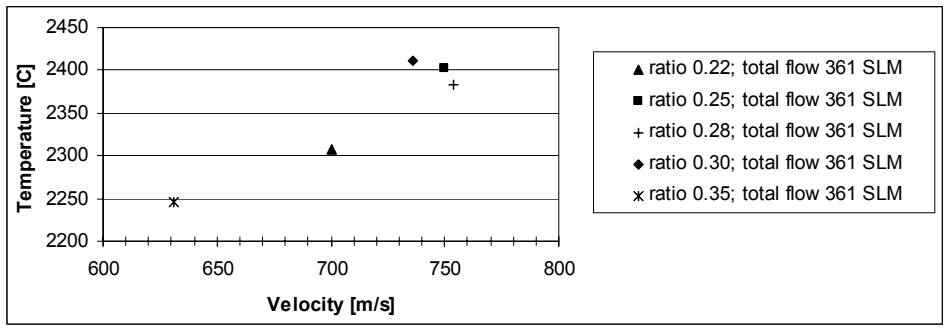

a)

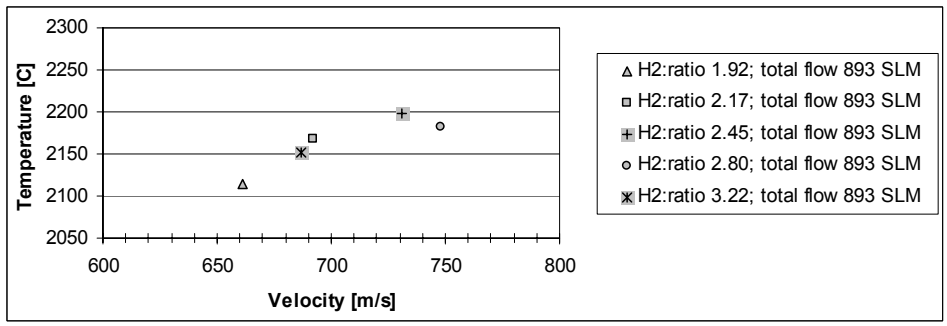

b)

Figure 7. Process diagnostic data for different spray parameter combinations: Effect of gas flow ratio.

The effect of combustion chamber length (22 mm and 19 mm) and the effect of changing the spray distance on the particles temperature-velocity spectrum are shown in Figure 8. Comparing the performance of combustion chambers, it is clear that the length has a significant effect on the particle temperature, but not on the velocity. Longer nozzle length seemed to allow for better combustion of gases and heat transfer to the particles, thereby raising the temperature, but velocity is influenced more by the throughput of gases.

The effect of standoff distance on particle conditions was examined for three different spray distances. As seen in Figure 8, the highest velocity and temperature point was that measured at the shortest spray distance (150 mm), the one with medium values at 175 mm, and the lowest velocity and temperature point at 200 mm.

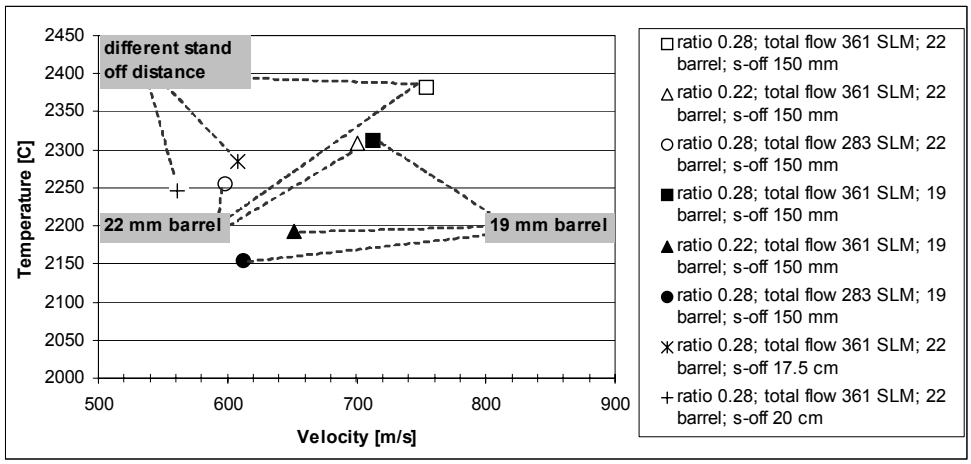

Figure 8. Process diagnostic data for different spray parameter combinations: Effect of barrel length and standoff distance.

3.2.2 Single splat studies

3.2.2.1 Alumina

Single splat studies were carried out for certain selected spray conditions. Large variations in the melting states were obtained under different conditions. Some of the main trends are presented in Figure 9.

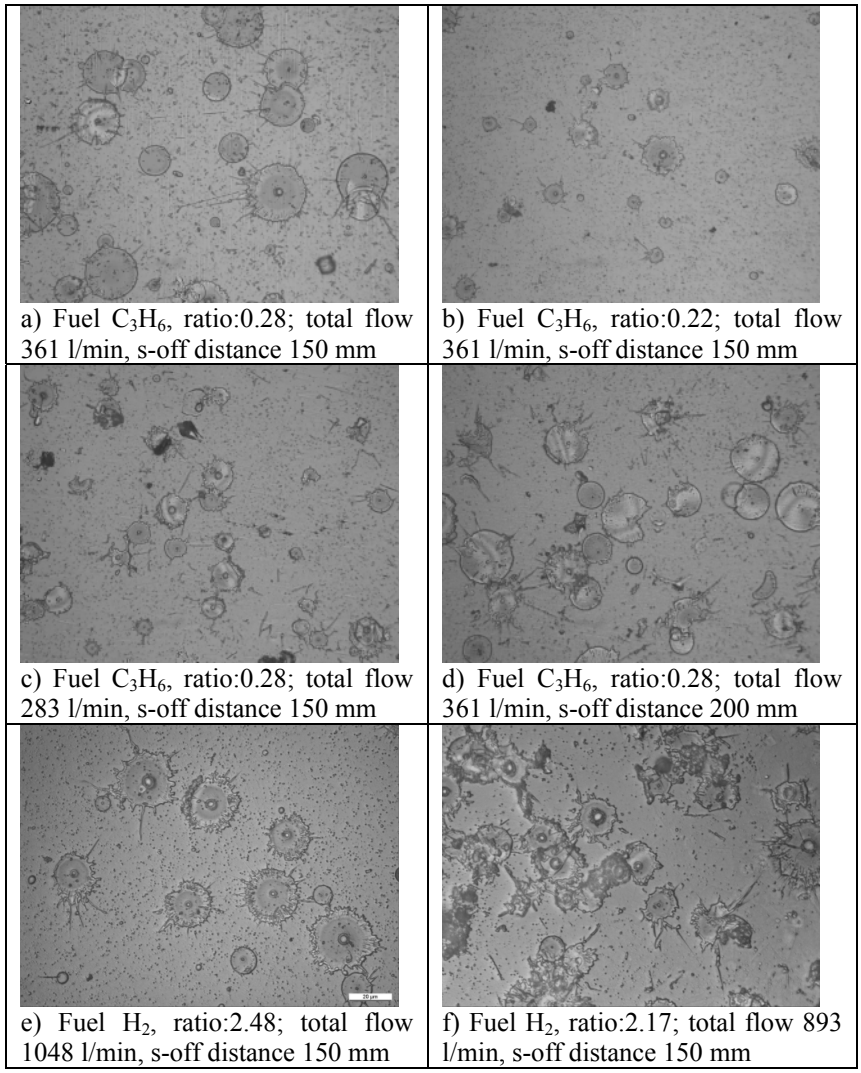

a) Fuel C_3H_6, ratio:0.28; total flow 361 l/min, s-off distance 150 mm

b) Fuel C_3H_6, ratio:0.22; total flow 361 l/min, s-off distance 150 mm

c) Fuel C_3H_6, ratio:0.28; total flow 283 l/min, s-off distance 150 mm

d) Fuel C_3H_6, ratio:0.28; total flow 361 l/min, s-off distance 200 mm

e) Fuel H_2, ratio:2.48; total flow 1048 l/min, s-off distance 150 mm

f) Fuel H_2, ratio:2.17; total flow 893 l/min, s-off distance 150 mm

Figure 9. Micrographs depicting the morphology of the alumina splats collected at different spray parameters. The parameters are explained in detail in Table 4.

Different temperature-velocity points were selected to investigate the effect of the particle surface temperature on the melting behavior of the particle. Particle wetting and flattening is dependent on the particle conditions in the flame. The highest melting stage was obtained for the parameters detailed in Figure 9 (a), thus producing the highest temperature and velocity. A decrease in particle temperatures and velocities due to the changes in fuel gas/oxygen ratio decreased the extent of the melting of the particles (Figure 9 (b)).

The effect of particle flight time on the melting stage in the flame is demonstrated in Figures 9 (c) and (d). With these two parameters, the data obtained from diagnostic measurements were identical but at different stand off distances. Extended dwell time due to the higher standoff distance caused a better melting stage for the particles.

Figures 9 (e) and (f) present splats sprayed by using hydrogen as a fuel gas with two different total gas flows and ratios. Diagnostic studies showed that hydrogen gives slightly lower maximum particle temperatures, but higher velocities compared to propylene (Figure 9 (a)). Hydrogen fuel gas with a lower total gas flow rate (Figure 9 (f)) was selected for comparison of lower and higher particle temperature and velocity to the melting stage of the particle. Melting is good with both hydrogen parameters. In general, the use of hydrogen as a fuel gas resulted in a larger degree of fragmentation compared to the use of propylene as a fuel gas (compare Figures 9 (a) and (d)). This is attributed to increased particle velocities.

Splat thicknesses were analysed in more detail with three hydrogen conditions: those being A) 2.85–1,050 l/min-150 mm, B) 2.85–1,050 l/min-200 mm and C) 2.00–1,050 l/min-15 0mm. The average thickness was found to be 0.55 µm for condition A, 0.76 µm for condition B, and 0.48 µm for condition C. The results confirm the visual observations and diagnostic data, showing the lowest flattening at condition B due to the lowest particle temperature and velocity. Flattening of the particles increased (thickness decreased) with increasing particle velocity and temperature. The medians of the splat diameters were 19.25 µm for condition A, 18.8 µm for condition B, and 19.8 µm for condition C. As expected, the trend as, opposite to that of the diameters. Diameter was smallest with condition B, where splat thickness was highest. In all cases, the largest particles have not attached to the substrate. Partly, this is assumed to result from the polished surface, and partly from the semi-molten state of the larger particles.

3.2.2.2 Quasicrystals

Two fuel gas/oxygen ratios with a total flow of 900 l/min were selected for the splat studies. It was found that the powder melting state varies with the spray distance. Figure 10 is clear proof of this.

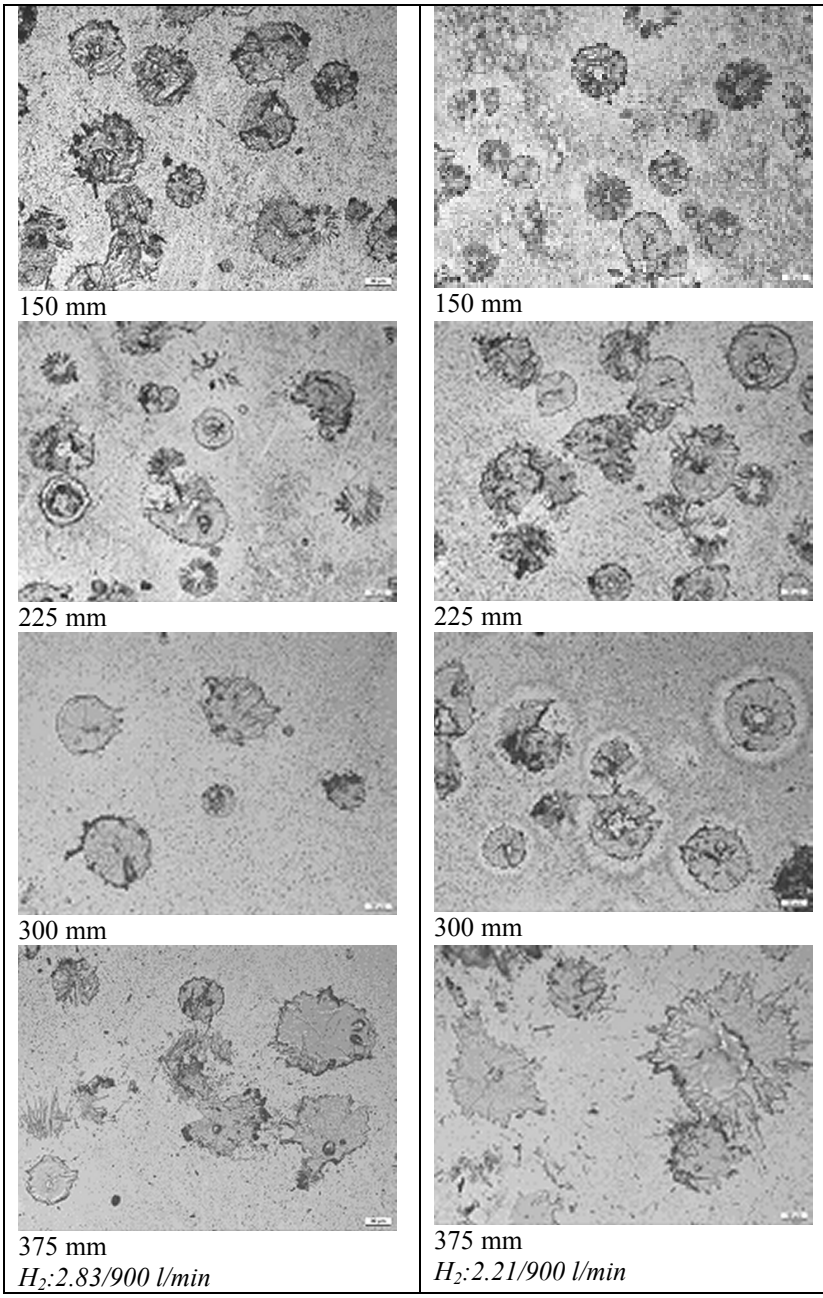

Figure 10. Illustration of the sprayed quasicrystal splats.

The melting stage of the particles when using a standoff distance of 300 mm is much higher than that produced with standoff distances of 150 mm and 225 mm. The shorter spray distances do not give enough time for the particles to melt. The melting was even more extensive with a spray distance of 375 mm, but this condition showed reduced particle flux, as well as low particle velocity, and cannot, therefore, result in good coating quality with a good deposition rate.

3.2.3 Coating characterization and properties

Alumina. Alumina coatings were produced from the powders presented in Chapter 2.1.

The coatings produced from commercial alumina powder with a conventional grain size have a clear correlation between their microstructure and the data obtained from the diagnostic tools. The best quality coatings were produced in conditions manifested by the highest particle temperature and velocity: a fuel gas /oxygen ratio of 0.28 with a total flow of 361 l/min for propylene, and a fuel gas /oxygen ratio of 2.48 with a total flow of 1050 l/min for hydrogen.

When working with agglomerated powder having a pure or composite nanofraction structure, the optimum spray conditions were slightly shifted from the ratio of 2.48. A stoichiometric fuel gas ratio (ratio 2.00) and ratio of 2.85 produced coatings with a highest density. Both conditions representing slightly lower particle temperatures compared with the ratio of 2.48. While working with nanostructured powders, the optimal spray condition should include sufficient melting without overheating combined with high particle velocity. Based on the splat studies, melting was sufficient with the gas ratios of 2.00 and 2.85. This can be assumed to result from the agglomerated powder structure. Condition 2.48, which was found to be best for the fused and crushed reference powder, caused a large amount of fragmentation, which can in turn be assumed to decrease coating uniformity. In the case of the agglomerated structure, a fuel-rich condition with a ratio of 2.85 was found to result in the best quality coatings ranked on the microstructure and wear behavior.

Increasing the spray distance was found to degrade the quality of the coating microstructure, resulting in a coating with higher porosity and poor flattening of

the particles. The differences in the microstructures are presented in Figure 11. These are micrographs from polished cross sections obtained by SEM in BEI mode in order to ensure a good contrast for illustrating the flattening stage and coating microstructure.

In all cases the amount of alpha phase was very low because of the high melting level of the particles. For n-Al_2O_3 powder the α/γ ratio was 9%/91% for a coating of 2.85–1050 l/min-150mm, 8%/82% for a coating of 2.85–1050 l/min-200mm, and 3%/97% for a coating of 2.00–1050 l/min-150mm.

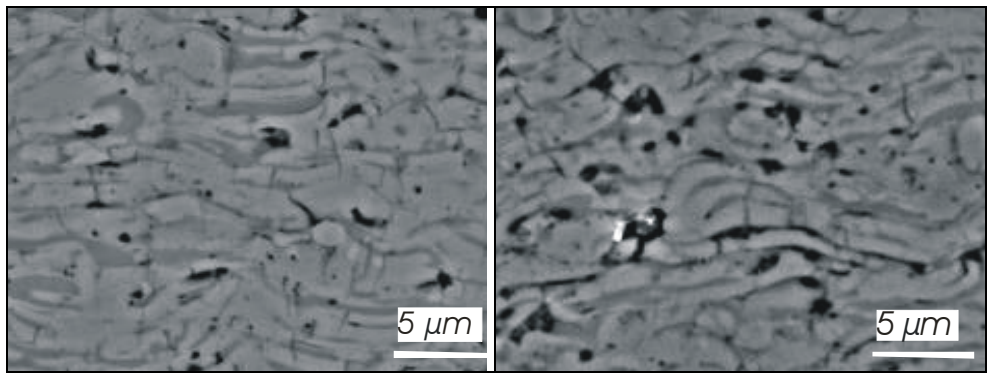

Figure 11. Effect of the standoff distance on the coating microstructure a) 150 mm, b) 200 mm.

A coating microstructure inside one lamella was studied by high resolution SEM. A high resolution SEM image of the fracture surface of an n-Al_2O_3 coating (2.00–1,050 l/min-150 mm) is shown in Figure 12. Alumina grains with dimensions in a range of hundreds of nanometers are observed. It should be noted that the fine structure seems to have been retained in spite of extensive melting of the powder in the HVOF process and only a small amount of α-Al_2O_3 in the structure.

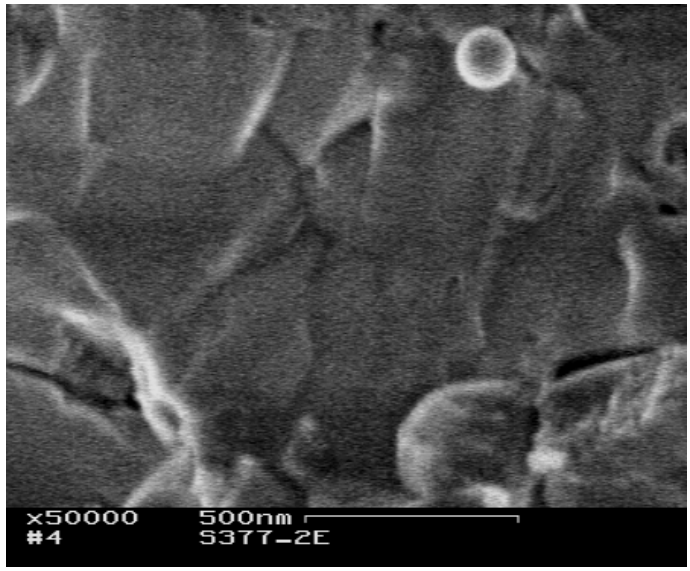

Figure 12. An FEG-SEM micrograph of a fracture surface of an n- Al_2O_3 - HVOF coating.

Some differences in the coating microstructure were observed for the Ni-alloyed nanostructured composite coatings between spray conditions with a ratio of 2.00 and a ratio of 2.85. The distribution of nickel in the polished cross sections of the samples as revealed by the back-scattered electron imaging is shown in Figures 13 (a) and (b). These micrographs indicate that nickel is partly deposited into the splat boundaries, i.e. interlamellarily. A coating sprayed with a ratio of 2.00 has a lower amount of nickel transferred to the lamella boundaries.

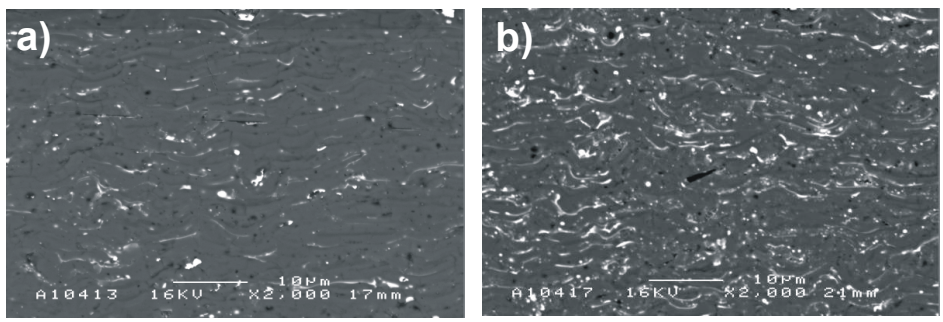

Figure 13. SEM-BEI micrograph of the polished cross sections for the coatings sprayed with different spray parameters a) n-Al_2O_3-5%Ni (ratio 2.00), b) n-Al_2O_3-5%Ni (ratio 2.85).

Different mechanical properties were determined for alumina coatings, including hardness, abrasive wear resistance and elastic modulus. Some electrical properties were also studied, including dielectric constant and breakdown strength. Figure 14 summarizes some results.

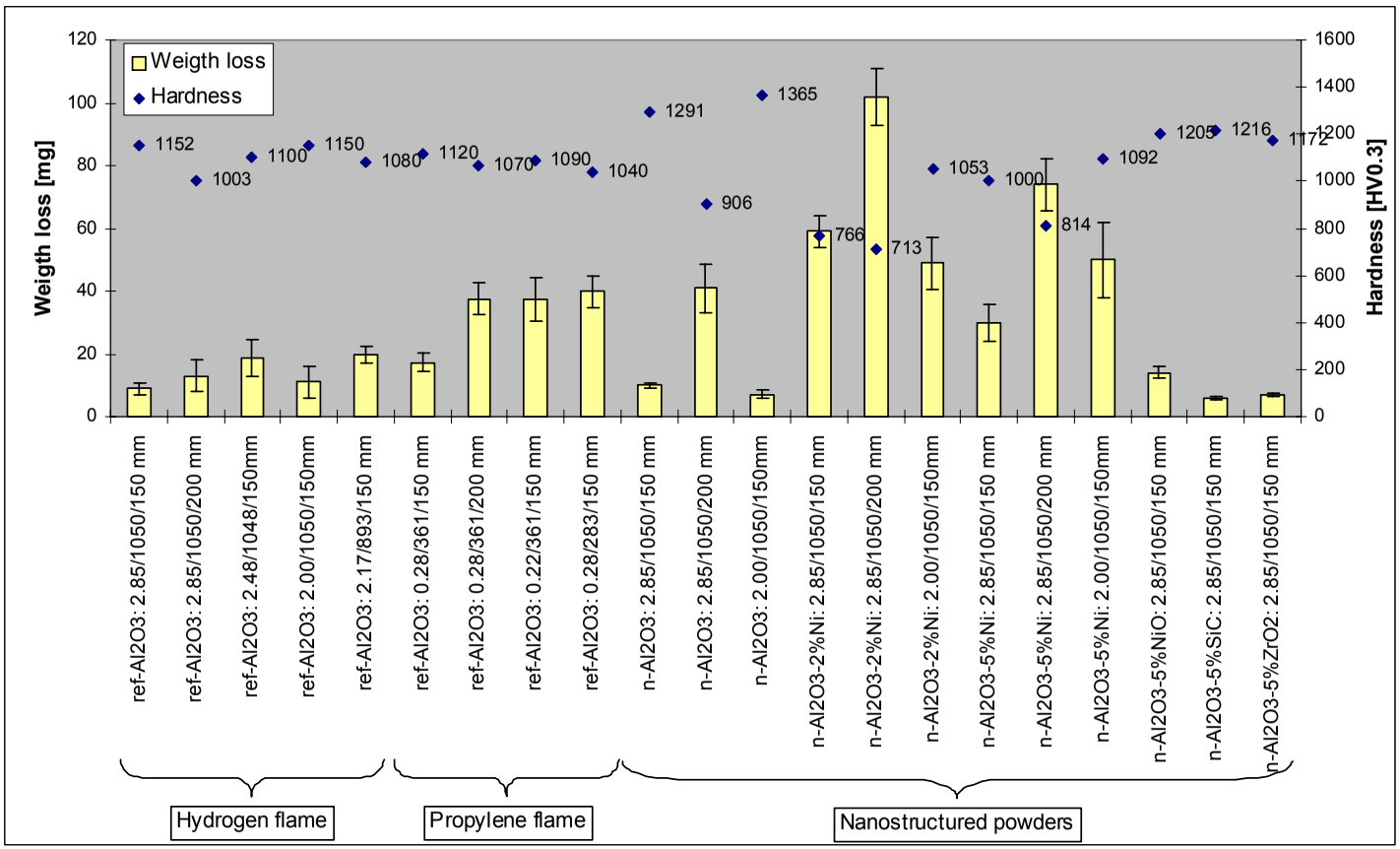

Figure 14. Hardness and weight loss in the abrasive rubber wheel wear test measurements for different alumina coatings.

Quasicrystals. The microstructure and the phase structure were studied for the coatings sprayed with the parameters detailed in the Table 5. It was found that dense and well-bonded coatings with partially or almost 100% quasicrystalline microstructures could be obtained, depending on the coating material. The main differences in the coatings made using spray parameters A and B were in the amount of porosity and oxidation of the particles.

It was concluded from the differences in the phase transformation and coating structure optimization between the different powders that the *Al-Cu-Fe* coating (F1) could only be deposited with a partially quasicrystalline coating consisting of quasicrystalline icosahedral i-$Al_{65}Cu_{20}Fe_{15}$ and crystalline cubic β-AlFe phases. The main difference between the two conditions was the formation of a thicker oxide layer with parameter A. An *Al-Cu-Fe-Cr* coating (A1/S) also formed a two-phase structure, but in this case both phases were quasicrystalline: $Al_{80}Cr_{13,5}Fe_{6,5}$ and $Al_{13}Cr_3Cu_4$. The *Al-Co-Fe-Cr* coating (BT1) was most interesting and consisted of the very rarely reported dodecagonal phase $Al_{70.6}Co_{12.5}Fe_{9.4}Cr_{7.5}$.

It was found that the Al-Cu-Fe alloy (F1) was the most sensitive to phase transformations, Al-Cu-Fe-Cr (A1/S) formed two different phases, but was mainly quasicrystalline, and Al-Co-Fe-Cr (BT1) was the most stable and fully quasicrystalline with a wide range of process parameters.

Relatively high values of the coefficient of friction (CoF) were obtained in the PoD test. These tests yielded friction values typically varying between 0.4–0.6, independent of the counter material. While the coefficient of friction was unexpectedly high at low temperatures, it seemed that increasing the temperature up to 500 °C did not increase the CoF. This is an encouraging result regarding the possible high-temperature use of these coatings. Based on the results, it can be concluded that the material is very stable up to relatively high temperatures, and no change in tribological behavior was recorded.

Interesting results were obtained in torsional testing of the coatings with various counter materials. In general, friction appeared to depend on the contact pressure induced, but not in a straightforward manner as depicted in Figure 15. During the tests, the contact pressure was varied between 5 and 15 MPa. The coefficient of friction increased first with the increased surface pressure being highest (0.35)

at the pressure of 10 MPa. A further increase in surface pressure decreased CoF close to the starting value (approx. 0.25). When the surface pressure was adjusted back to 10 MPa, the measured CoF was much lower (0.18–0.23) compared to the previously measured values. The history-dependence of the friction seems to indicate that pressure-dependent changes occur in the tribofilm. In certain circumstances this seems to be very beneficial when friction decreases with increasing pressure.

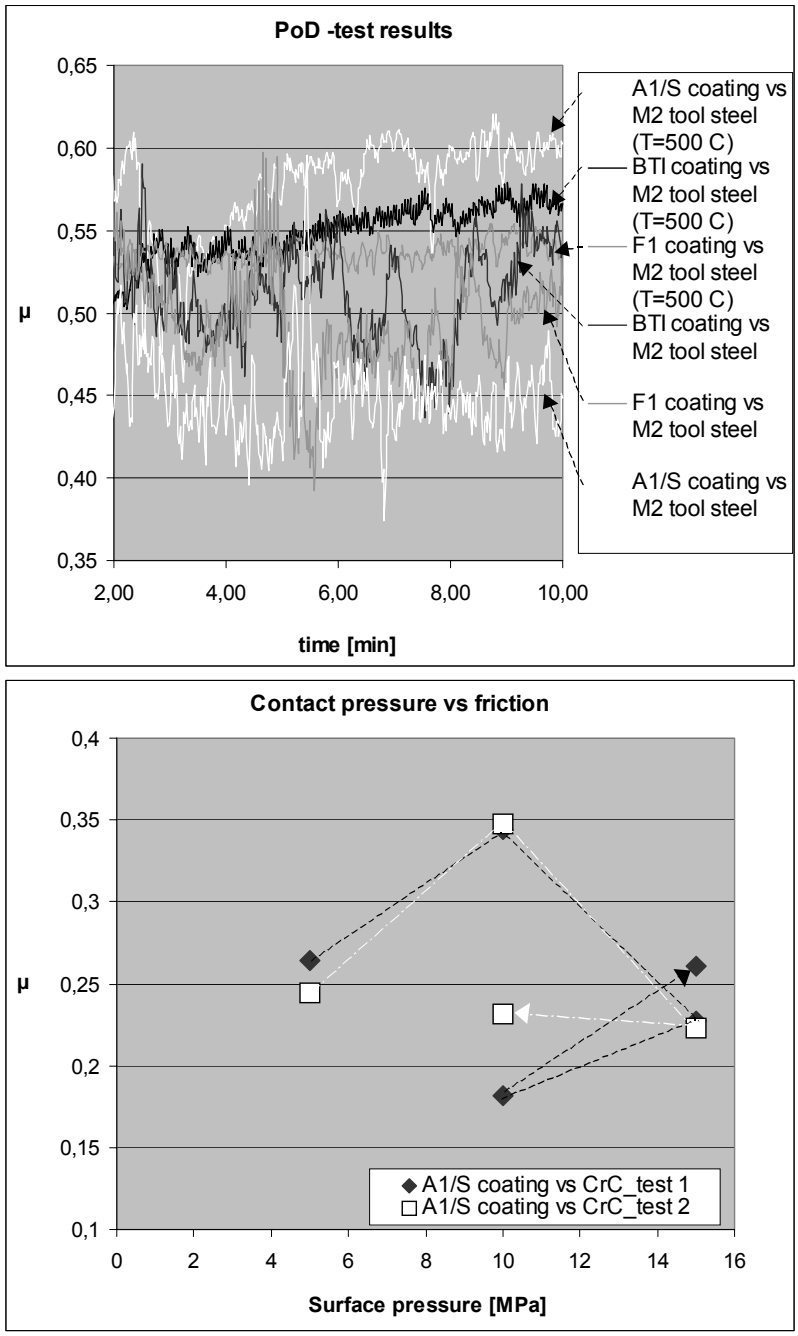

Figure 15. a) PoD test of the QC coatings against M2 steel, b) average friction v. contact pressure in A1/S-Cr_3C_2-NiCr contact.

4. Discussion

Detailed on-line diagnostic studies were carried out on HVOF-sprayed alumina coatings for the first time. These were based on investigation of the fuel gas/oxygen ratio and total gas flow effect on the coating structure.

Diagnostic studies confirmed the findings of Lugscheider[31, 36] and Hanson[37] who proposed that hydrogen produces particles with higher velocity and lower temperatures. Therefore, hydrogen can be considered a more optimal fuel gas when spraying materials that are sensitive to overheating. On the other hand, use of propylene offers a wider process window in terms of particle temperature and velocity, and allows more variation in the process conditions. Normally this can be considered to increase the risks in process reliability, but in some special cases this can be also considered to offer more possibilities to affect the coating structure.

Total gas throughput has a straightforward effect on the gas velocity. An increase in total gas flow increases both particle velocity and temperature at a certain fuel gas/oxygen ratio. This correlates well with the findings of Planche[38].

Maximum temperature was obtained with fuel-rich conditions – 0.25–0.30 for propylene-oxygen ratios and 2.45–2.85 for hydrogen-oxygen ratios – in the case of alumina. It was also recognized that maximum particle velocities inside one total gas flow were nearly always obtained at the same time as maximum temperatures.

Particle velocity is clearly dependent on the spray distance, this being highest with a short spray distance. In the case of alumina the decrease in velocity was 25% when the standoff distance increased from 150 mm to 200 mm. In the case of quasicrystals the decrease was 10–20% when the standoff distance increased from 150mm to 225 mm. The difference is correlated to the weight of the particles. Due to the higher weight of the quasicrystal particles, the decrease in velocity is not as high as that of the alumina particles. The effect of the standoff distance on the particle temperature was different for alumina and QCs. In the case of alumina the measured temperatures decreased by 5% due to the growth in the spray distance. In the case of quasicrystals the temperature rose 1–2% with standoff distances of 150 mm to 225 mm and were highest at the longest

spray distance of 375 mm. The behavior of the QCs correlates well with the findings of Lugscheider for MCrAlY materials[36]. The reduction in temperatures with alumina powder can be assumed to result from the poorer flight properties of the smallest alumina particles. Thus larger particles with a lower surface temperature were measured at greater distances.

Splat formation correlated well with the diagnostic studies. The melting stage was typically most advanced at the highest temperatures. However, the dwell time had an effect on the melting stage, which cannot be directly observed from the diagnostic studies. An increased standoff distance with "hotter" flame parameters resulted in a higher melting stage for the particles compared with a lower standoff distance and "colder" flame parameters. Still, these two conditions gave equal particle velocity-temperature data in the diagnostic studies. This is a clear example of the fact that information obtained from the on-line diagnostics gives only the v/T data for the particle in a certain position and does not take into account the v/T -history concerning what the particle has gone through previously.

The microstructure of the alumina coating was related to the particle velocities and the melting stage of the particles. In the case of pure alumina with a conventional grain size, the maximum melting of the particle was expected to produce a dense coating. Figure 16 summarizes the findings. Measured particle velocity and temperature data is plotted against coating abrasive wear resistance and hardness. A weight loss of 20 mg and hardness of HV 1,100 were taken for the limits. The formed first order process map shows the clear correlation between particle melting behavior and the abrasive wear resistance and the hardness. The process map shows that by using hydrogen as a fuel gas, higher variations in spray conditions are tolerated in order to produce a coating with good wear resistance. The change in hardness was slightly more sensitive for hydrogen gas flows. A decrease in particle velocity is assumed to have an effect on the lamella adhesion.

A wider melting spectrum was obtained for propylene. Due to this, the number of process conditions producing the high temperature suitable for sufficient alumina melting is lower than that for hydrogen. This results in a much narrower window for optimal spray parameters when working with propylene as a fuel gas.

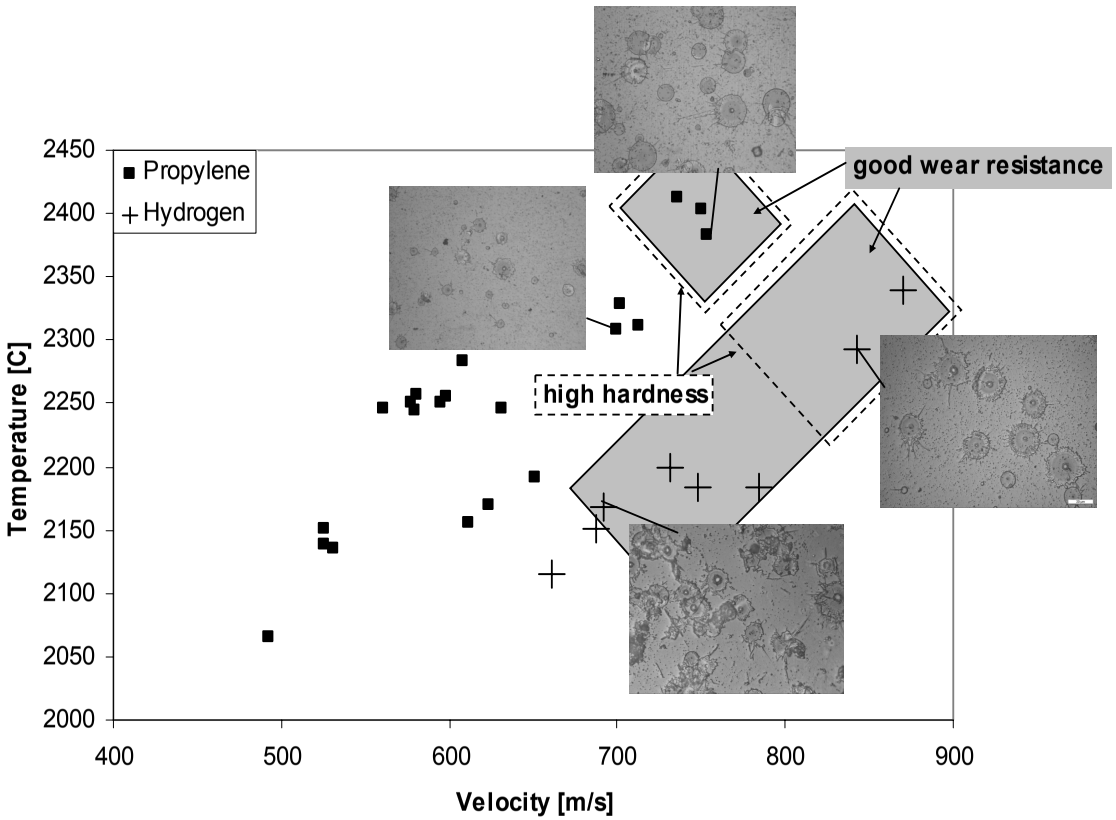

Figure 16. The first order process map for alumina plotted against wear resistance and hardness of the produced coatings.

With nanostructured alumina the coating microstructure and mechanical properties also correlated strongly with the particle melting stage. It was recognized that it is not possible to improve the mechanical properties of the entire coating without sufficient interlamellar adhesion, despite the desired microstructure and crystal size of one lamella. Therefore, the interlamellar adhesion is dominant for the mechanical properties of the coating and must be prioritized in the parameter selection. The obtained results correlated with the results published for APS sprayed nanostructure alumina-titania coatings, where obtained hardness values are reported to be in the range of 1,100 $HV_{0.3}$.[75]

The studies showed that the coating microstructure can be estimated from the diagnostic data and splat studies. Due to the coarser particle size of the quasicrystalline materials, and their higher density, the standoff distance for optimal coating formation was much higher than that for alumina; 300 mm was found to be optimal. The two selected conditions did not markedly change the coating structure. The main difference between the two parameters was the thickness of the oxidation layer for composition *Al-Cu-Fe* being higher for condition A, which is a more oxygen-rich condition than that of condition B. A similar trend was observed with the composition *Al-Co-Fe-Cr*, where the oxygen-rich condition produced a higher amount of oxidation. Introducing chromium into the structure (composition *Al-Cu-Fe-Cr*) increased the amount of quasicrystalline phases and was concurrently reflected in the negligible oxidation. It must be noted that the particle temperature and velocities were not actually varied much compared with the dwell time of the particle in the flame due to the long standoff distance. Therefore, no large differences in particle melting behavior between the two conditions can be expected. The formed coating structure was in agreement with the earlier studies made by APS spraying for the same type of composition, although HVOF spraying produced a coating with less porosity.

5. Summary and conclusions

Diagnostic tools, including on-line diagnostic and single splat studies, were shown to be an effective tool for the process optimization of the HVOF spray process. The usability of diagnostic tools was demonstrated when working with materials having a narrow processing window with regard to melting and degradation temperatures.

It was shown that diagnostic results can be correlated with the coating microstructure and coating properties in HVOF spraying. It was also demonstrated that the coating properties and coating quality can be improved by optimizing and carefully selecting the spray parameters.

This work concentrated on the optimization of the micro and phase structure of the coating. It must be pointed out that control of the internal stresses of the coating is also essential in order to develop high-performance coatings.

It was clearly pointed out during the work that the coating density, including splat flattening and interlamellar adhesion, is important in order to produce high-performance coatings and that it must be prioritized in the coating parameter optimization.

References

[1] Davis, J.R. (Ed.). Handbook of Thermal Spray Technology. Thermal Spray Society, ASM International, Materials Park, OH, USA (2004), p. 338.

[2] Heinrich, P. Thermal spraying – Facts and state of the art. Sonderdruck, E10/92 (1992), p. 28.

[3] Pawlowski, L. The science and engineering of thermal spray coatings. John Wiley & Sons, New York, NY, USA (1995), p. 432.

[4] Kulkarni, A., Gutleber, J., Sampath, S., Goland, A., Lindquist, W.B., Herman, H., Allen, A.J. & Dowd, B. Studies of the microstructure and properties of dense ceramic coatings produced by high-velocity oxygen-fuel combustion spraying. Materials Science and Engineering A369(2004), pp. 124–137.

[5] Ramm, D.A.J., Clyne, T.W., Sturgeon, A.J. & Dunkerton, S. Correlations between spraying conditions and microstructure for alumina coatings produced by HVOF and VPS. Proceedings of the 7th National Thermal Spray Conference, 20–24 June, 1994, Boston, Massachusetts, USA (1994, pp. 239–244.

[6] Sturgeon, A.J., Harvey, M.F.D. & Blunt, F.J. The influence of fuel gas on the microstructure and wear performance of alumina coatings produced by the High Velocity Oxyfuel (HVOF) thermal spray process. British Ceramic Proceedings, Vol. 54(1997), pp. 57–64.

[7] Sturgeon, A.J. Recent advantages and applications of thermal sprayed ceramic coatings, British Ceramic proceedings, Vol. 55(1996), pp. 3–12.

[8] Sampath, S., Jiang, X., Kulkarni, A., Matejicek, J., Gilmore, D.L. & Neiser, R.A. Development of process maps for plasma spray: case study for molybdenum. Materials Science and Engineering A348(2003), pp. 54–66.

[9] Kreye, H., Schwetzke, R. & Zimmermann, S. High velocity oxy-fuel flame spraying process and coating characteristics. Thermal Spray: Practical solutions for Engineering Problems. Berndt, C.C. (Ed.). Published by ASM International, Materials Park, Ohio-USA (1996), pp. 451–456.

[10] Li, M., Shi, D. & Christofides, P.D. Model-based estimation and control of particle velocity and melting in HVOF thermal spray. Chemical Engineering Science 59(2004), pp. 5647–5656.

[11] Dubsky, J. & Matějiček, J. Residual and applied stresses in thermally sprayed metallic and ceramic coatings, Thermal Spray 2002. Proceedings, International Thermal Spray Conference (ITSC 2002), Essen, 4–6 March 2002. Lugscheider, E. (Ed.). (2002), pp. 606–609.

[12] Allen, A.J., Long, G.G., Boukari, H., Ilavsky, J., Kulkarni, A., Sampath, S., Herman, H. & Goland, A.N. Microstructural characterization studies to relate the properties of thermal spray coatings to feedstock and spray conditions. Surface and Coatings Technology, 146–147(2001), pp. 544–552.

[13] Friis, M. & Persson, C. Control of thermal spray process by means of process maps and process windows. Journal of Thermal Spray Technology, 12, 1(2003), pp. 44–52.

[14] Nylén, P., Lemaitre, J. & Wigren, J. Sensitivity of four on-line diagnostic systems for plasma spraying. Thermal spray 2003: Advancing the science and applying technology. Moreau, C. & Marple, B. (Eds.). Published by ASM International, Materials Park, Ohio-USA (2003), pp. 1101–1106.

[15] Steffens, H.-D. & Duda, T. Enthalpy measurement of direct current plasma jets used for ZrO_2-Y_2O_3 thermal barrier coatings. Journal of Thermal Spray Technology, 9, 2(2000), pp. 235–240.

[16] Tucker, R.C. Jr. Integrated thermal spray systems – some practical considerations. Thermal spray 2001: New surfaces for a new millennium. Berndt, C.C., Khor, K.A. & Lugscheider, E.F. (Eds.). Published by ASM International, Materials Park Ohio, USA (2001), pp. 1261–1266.

[17] Hämäläinen, E., Vattulainen, J., Alahautala, T., Hernberg, R., Vuoristo, P. & Mäntylä, T. Imaging diagnostics in thermal spraying – "SprayWatch" system. Thermal Spray Surface Engineering via Applied Research, Proceedings, 1st International Thermal Spray Conference (ITSC 2000), Montreal, Quebec, Canada; 8–11 May 2000, pp. 79–83.

[18] Fincke, J.R., Swank, W.D., Bewley, R.L. & Haggard, D.C. Control of particle temperature, velocity, and trajectory in thermal spray process. Thermal spray 2003: Advancing the science and applying technology. Moreau, C. & B. Marple, B. (Eds.). Published by ASM International, Materials Park, Ohio-USA (2003), pp. 1093–1099.

[19] Moreau, C., Gougeon, P., Lamontagne, M., Lacasse, V., Vaudreuil, G. & Cielo, P. On-line Control of the Plasma Spraying Process by Monitoring the Temperature, Velocity and Trajectory of In-Flight Particles. Proceedings of the 7th National Thermal Spray Conference 20–24 June 1994, Boston, USA (1994), pp. 431–437.

[20] Fincke, J.R., Haggard, D.C. & Swank, W.D. Particle Temperature Measurement in the Thermal Spray Process. Journal of Thermal Spray Technology, 10, 2(2001), pp. 255–266.

[21] Vuoristo, P., Ahmaniemi, S., Nuutinen, S., Mäntylä, T., Hämäläinen, E., Arola, N. & Vattulainen, J. Optimisation and monitoring of spray parameters by a CCD camera based imaging thermal spray monitor. Thermal spray 2001: New surfaces for a new millennium. Berndt, C.C., Khor, K.A. & Lugscheider, E.F. published by ASM International, Materials Park Ohio, USA (2001), pp. 727–736.

[22] Lugscheider, E., Fischer, E., Koch, D. & Papenfuß, N. Diagnostics of in flight particle properties and resulting coating qualities on atmospheric plasma process, Thermal Spray 2001. New Surfaces for a New Millennium, Proceedings, International Thermal Spray Conference (ITSC 2001), Singapore; 28–30 May 2001, pp. 751–758.

[23] Bianchi, L., Blein, F., Lucchese, P., Vardelle, M., Vardelle, A. & Fauchais, P. Effect of particle velocity and substrate temperature on alumina and zirconia splat formation. Proceedings of the 7th National Thermal Spray Conference 20–24 June 1994, Boston, USA (1994), pp. 569–574.

[24] Fan, X., Gitzhofer, F. & Boulos, M. Investigation of alumina splats formed in the induction plasma process. Journal of Thermal Spray Technology, Vol. 7, No. 2, June 1998, pp. 197–204.

[25] Fauchais, P., Vardelle, A., Vardelle, M., Denoirjean, A., Pateyron, B. & El Ganaoui, M. Formation and layering of alumina splats: thermal history of coating formation, resulting stresses and coating microstructure. Thermal Spray 2001. New Surfaces for a New Millennium, Proceedings, International Thermal Spray Conference (ITSC 2001), Singapore; 28–30 May 2001, pp. 865–873.

[26] Fukanuma, H. & Ohmori, A. Behaviour of molten droplets impinging on flat surfaces, Effect of particle velocity and substrate temperature on alumina and zirconia splat formation. Proceedings of the 7th National Thermal Spray Conference 20–24 June 1994, Boston, USA (1994), pp. 563–568.

[27] Sampath, S. & Jiang, X. Splat formation and microstructure development during plasma spraying: deposition temperature effects. Materials Science and Engineering A304–306 (2001), pp. 144–150.

[28] Vardelle, M., Vardelle, A., Leger, A.C. & Fauchais, P. Dynamics of splat formation and solidification in thermal spraying process. Proceedings of the 7th National Thermal Spray Conference 20–24 June 1994, Boston, USA (1994), pp. 555–562.

[29] Sundararajan, G., Sivakumar, G. & Srinivasa Rao, D. The interrelationship between particle velocity and temperature, spalt formation and deposition efficiency in detonation sprayed alumina coatings. ITSC 2001: International Thermal Spray Conference 2001, Singapore; 28–30 May 2001, pp. 849–858.

[30] Hackett, C.M. & Settles, G.S. Independent control of HVOF particle velocity and temperature, Thermal Spray: Practical solutions for Engineering Problems. Berndt, C.C. (Ed.). Published by ASM International, Materials Park, Ohio-USA (1996), pp. 665–673.

[31] Lugscheider, E., Herbst-Dederichs, C. & Zhao, L. Particle behavior in a powder-laden HVOF jet. ITSC 2000: 1st International Thermal Spray Conference; Montreal, Quebec; Canada; 8–11 May 2000, pp. 501–508.

[32] Yamada, H., Kuroda, S., Fukushima, T. & Yumoto, H. Capture and evaluation of HVOF thermal sprayed particles by a gel target. ITSC 2001: International Thermal Spray Conference 2001, Singapore; 28–30 May 2001, pp. 797–-804.

[33] Sobolev, V.V., Guilemany, J.M. & Martin, A.J. Engineering Formulas for flattening of composite particles during thermal spraying. Thermal Spray, A united forum for scientific and technological advances, ASM international (1997), 653–656.

[34] Sobolev, V.V. & Guilemany, J.M. Formation of splats during thermal spraying of composite powder particles. Materials Letters 42(2000), pp. 46–51.

[35] Sampath, S., Jiang, X.Y., Matejicek, J., Prchlik, L., Kulkarni, A. & Vaidya, A. Role of thermal spray processing method on the microstructure, residual stress and properties of coatings: an integrated study for Ni-5 wt.%Al bond coats. Materials Science and Engineering A364(2004), pp. 216–231.

[36] Lugscheider, E., Herbst, C. & Zhao, L. Parameter studies on high-velocity oxy-fuel spraying of MCrAlY coatings. Surface and coatings technology 108–109(1998), pp. 16–23.

[37] Hanson, T.C. & Settles, G.S. Particle temperature and velocity effects on the porosity and oxidation of an HVOF corrosion-control coating. Journal of thermal spray technology 12, 3(2003), pp. 403–415.

[38] Planche, M.P., Normand, B., Liao, H., Rannou, G. & Coddet, C. Influence of HVOF spraying parameters on in-flight characteristics of Inconel 718 particles and correlation with the electrochemical behaviour of the coating. Surface and coatings technology 157(2002), pp. 247–256.

[39] Gil, L. & Staia, M.H. Influence of HVOF parameters on the corrosion resistance of NiWCrBSi coatings. Thin solid films 420–421(2002), pp. 446–454.

[40] Li, M. & Christofides, P.D. Multi-scale modelling and analysis of an industrial HVOF thermal spray process. Chemical engineering science 60 (2005), pp. 3649–3669.

[41] Li, M., Shi, D. & Christofides, P.D. Diamond jet hybrid HVOF thermal spray: gas-phase and particle behaviour modeling and feedback control design. Industrial and engineering chemistry research 43(2004), pp. 3632–3652.

[42] Shi, D., Li, M. & Christofides, P.D. Diamond jet hybrid HVOF thermal spray: rule-based modelling of coating microstructure. Industrial and engineering chemistry research 43(2004), pp. 3653–3665.

[43] Dolatabadi, A., Pershin, V. & Mostaghimi, J. Effect of flow regime on particle velocity in the high velocity oxyfuel (HVOF) [spraying] process, Thermal Spray 2002. Proceedings, International Thermal Spray Conference (ITSC 2002), Essen, 4–6 March 2002. Lugscheider, E. (Ed.). Publ: 40010 Dusseldorf, Germany; DVS-Verlag, for Deutscher Verband fur Schweissen und verwandte Verfahren; 2002, pp. 918–925.

[44] Hackett, C.M., Settles, G.S. & Miller, J.D. On the gas dynamics of HVOF thermal sprays. Journal of Thermal Spray Technology 3(3) Sept. 1994, pp. 299–304.

[45] Hearley, J.A., Little, J.A. & Sturgeon, A.J. The effect of spray parameters on the properties of high velocity oxy-fuel NiAl intermetallic coatings. Surface and coatings technology 123(2000), pp. 210–218.

[46] Ignatiev, M., Smurov, I. & Bertrand, P. Application of digital CCD camera for monitoring of particle-in-flight parameters in plasma and HVOF spraying, Thermal Spray 2002. Proceedings, International Thermal Spray Conference (ITSC 2002), Essen, 4–6 March 2002. Lugscheider, E. (Ed.). DVS-Verlag, for Deutscher Verband für Schweissen und verwandte Verfahren; Dusseldorf, Germany (2002), pp. 72–77.

[47] Bertrand, P., Smurov, I. & Ignatiev, M. Low cost industrial type diagnostic system for powder jet visualisation, particle-substrate interaction and coating growth, Thermal Spray 2002. Proceedings, International Thermal Spray Conference (ITSC 2002), Essen, 4–6 March 2002. Lugscheider, E. (Ed.). DVS-Verlag, for Deutscher Verband fur Schweissen und verwandte Verfahren; Dusseldorf, Germany; (2002), pp. 66–71.

[48] Arsenault, B., Legoux, J.G., Hawthorne, H., Immarigeon, J.P., Gougeon, P. & Moreau, C. HVOF process optimization for the erosion resistance of WC-12Co and WC-10Co-4Cr coatings. ITSC 2001: International Thermal Spray Conference 2001, Singapore; 28–30 May 2001, pp. 1051–1060.

[49] Devasenapathi, A., Shimizu, Y., Kazuhiko, S. & Minamida, T. Effect of spraying parameters on the microstructure of alumina coating sprayed by high velocity oxyfuel (HVOF) method. Nippon Yosha Kyokai Shi (Journal of Japan Thermal Spraying Society), 36, 1(1999), pp. 1–11.

[50] Lima, R.S. & Marple, B.R. Fro APS to HVOF spraying of conventional and nanostructured titania feedstock powders: a study on the enhancement of the mechanical properties. Surface and coatings technology (2004) article in press, available online (http://www.sciencedirect.com)

[51] Saravanan, P., Selvarajan, V., Rao D.S., Joshi, S.V. & Sundararajan, G. Influence of process variables on the quality of detonation gun sprayed alumina coatings. Surface and coatings technology 123(2000), pp. 44–54.

[52] Niemi, K., Vuoristo, P., Kumpulainen, E., Sorsa, P. & Mäntylä, T. Recent Developments in the Characteristics of Thermally Sprayed Oxide Coatings. Proceedings of 14th international thermal spray conference, 22–26 May 1995, Kobe, Japan (1995), p. 687–694.

[53] Liu, Y., Fischer, T.E. & Dent, A. Comparison of HVOF and plasma sprayed alumina/titania coatings-microstructure, mechanical properties and abrasion behaviour. Surface and Coatings Technology 167(2003), pp. 68–76.

[54] Kadyrov, V., Evdokimenko, Y., Kisel, V. & Kadyrov, E. Calculation of the limiting parameters for oxide ceramic particles during HVOF spraying. Proceedings of the 7th National Thermal Spray Conference 20–24 June, 1994, Boston, Massachusetts, USA (1994), pp. 245–250.

[55] Sordelet, D.J., Besser, M.F. & Anderson, I.E. Particle size effects on chemistry and structure of Al-Cu-Fe quasicrystalline coatings. Journal of thermal spray technology 5, 2(1996), pp. 161–174.

[56] Lang, C.I., Shechtman, D. & Gonzalez, E. Friction and wear properties of quasi-periodic material coatings. Bull. Mater. Sci., 22(1999), pp. 189–192.

[57] Sordelet, D.J., Kramer, M.J., Anderson, I.E. & Besser, M.F. Microstructural evaluation, oxidation and wear of Al-Cu-Fe quasicrystalline coatings. Proceedings of the fifth international conference of quasicrystals (1995), pp. 778–785.

[58] De Palo, S., Usmani, S., Sampath, S., Sordelet, D.J. & Besser, M. Friction and wear behaviour of thermally sprayed Al-Cu-Fe quasicrystalline coatings. Thermal Spray, A united forum for scientific and technological advances, ASM international (1997), pp. 135–139.

[59] Fleury, E., Lee, S.M., Kim, W.T. & Kim, D.H. Effects of air plasma spraying parameters on the Al-Cu-Fe quasicrystalline coating layer. Journal of Non-Crystalline Solids 278(2000), pp. 194–204.

[60] Sordelet, D.J., Besser, M.F. & Kramer, M.J. Thermal spray quasicrystalline coatings. Part 1: relationship among processing, phase structure and splat morphology. Proceedings of the 15th international thermal spray conference, 25–29 May 1998, Nice, France (1998), pp. 467–471.

[61] Kuroda, S. Properties and characterisation of thermal sprayed coatings – a review of recent research progress. Proceedings of the 15th international thermal spray conference, 25–29 May 1998, Nice, France (1998), pp. 539–550.

[62] De Palo, S., Usmani, S., Kishi, K., Sampath, S., Sordelet, D.J. & Besser M.F. Thermal spray quasicrystalline coatings. Part II: relationships among processing, phase assemblage and tribological response. Proceedings of the 15th international thermal spray conference, 25–29 May 1998, Nice, France (1998), pp. 705–710.

[63] Anderson, C.W. & Heffner, K.H. Precision gas bearing plasma sprayed aluminium oxide coating characterization. Proceedings of the international thermal spray conference, Orlando, USA 28 May–5 June 1992, pp. 695–704.

[64] Ramachandran, K., Selvarajan, V., Ananthapadmanabhan, P.V. & Sreekumar, K.P. Microstructure, adhesion, microhardness, abrasive wear resistance and electrical resistivity of the plasma sprayed alumina and alumina-titania coatings. Thin Solid Films, 315, (1998), pp. 144–152.

[65] Swindeman, C.J., Seals, R.D., Murray, W.P., Cooper, M.H. & White, R.L. An investigation of the electrical behaviour of thermally sprayed aluminium oxide, Practical solutions for engineering problems. Berndt, C.C. (Ed.). ASM International, Materials Park, Ohio-USA (1996), pp. 793–797.

[66] Shackelford, J.F. Materials science and engineering handbook. Third edition, CRC press, Boca Raton, Florida, USA (2001), p. 1949.

[67] Levin, I., Bendersky, L.A., Brandon, D.G. & Rühle, M. Cubic to monoclinic phase transformations in alumina. Acta Mater. 9(1997), pp. 3659–3669.

[68] Devi, M.U. On the nature of phases in Al2O3 and Al2O3-SiC thermal spray coatings. Ceramics international 30(2004), pp. 545–553.

[69] Niemi, K., Vuoristo, P., Mäntylä, T., Lugscheider, E., Knuuttila, J. & Jungklaus, H. Wear characteristics of oxide coatings deposited by plasma spraying, high power plasma spraying and detonation gun spraying. Proceedings of the 8th national thermal spray conference, 11–15 September 1995, Houston, USA (1995), pp. 645–650.

[70] Hannula, S.-P., Koskinen, J., Haimi, E. & Nowak, R. Mechanical properties of nanostructured materials. Encyclopedia of Nanoscience and Nanotechnology, 5. Nalwa, H.S. (Ed.). American Scientific Publishers. California, USA (2004), pp. 31–162.

[71] Mayo, M.J. High and low temperature superplasticity in nanocrystalline materials. Nanostruct. Mater. 9(1997), pp. 717–726.

[72] Mohamed, F.A. & Li, Y. Creep and superplasticity in nanocrystalline materials: current understanding and future prospects. Mater. Sci. Eng. 298A(2001), pp. 1–15.

[73] Sekino, T., Nakajima, T. & Niihara, K. Mechanical and magnetic properties of nickel dispersed alumina-based nanocomposite. Materials letters 29(1996), pp. 165–169.

[74] Oh S.-T., Sando M. & Niihara K. Processing and Properties of Ni-Co Alloy Dispersed Al_2O_3 Nanocomposites. Scripta Materialia 39(1998), pp. 1413–1418.

[75] Shaw, L.L., Goberman, D., Ren, R., Gell, M., Jiang, S., Wang, Y., Xiao, T.D. & Strutt, P.R. The dependency of microstructure and properties of nanostructured coatings on plasma spray conditions. Surface and coatings technology 130(2000), pp. 1–8.

[76] Gell, M., Jordan, E.H., Sohn, Y.H., Goberman, D., Shaw, L. & Xiao, T.D. Development and implementation of plasma sprayed nanostructured ceramic coatings. Surface and Coatings Technology 146–147(2001), pp. 48–54.

[77] Jordan, E.H., Gell, M., Sohn, Y.H., Goberman, D., Shaw, L., Jiang, S., Wang, M., Xiao, T.D., Wang, Y. & Strutt, P. Fabrication and evaluation of plasma sprayed nanostructured alumina-titania coatings with superior properties. Mater. Sci. Eng. 301(2001), pp. 80–89.

[78] Goberman, D., Sohn, Y.H., Shaw, L., Jordan, E. & Gell, M. Microstructure development of Al_2O_3-13wt.%TiO_2 plasma sprayed coatings derived from nanocrystalline powders. Acta Materialia, 50(2002), pp. 1141–1152.

[79] Sordelet, D.J & Dubois, J.M. Quasicrystals: Perspectives and potential applications. MRS Bulletin, November 1997, pp. 34–37.

[80] Besser, M.F. & Eisenhammer, T. Deposition and applications of quasicrystal coating. MRS Bulletin, November 1997, pp. 59–64.

[81] Tamari, S. & Aguilar-Chàvez, A. Optimum Design of Gas Pycnometers for Determining the Volume of Solid Particles. Journal of Testing and Evaluation 33, 2(2005), p. 4.

[82] Field, J.S. & Swain, M.V. A Simple Predictive Model for Spherical Indentation. J. Mater. Res. 8, 2(1993), p. 297.

[83] Parker, W. Flash Method of Determining Thermal Diffusivity, Heat Capacity and Thermal Conductivity. J. Appl. Phys. 32, 9(1961), p. 1679.

Appendix I of this publication is not included in the PDF version.
Please order the printed version to get the complete publication
(http://www.vtt.fi/inf/pdf/)

Published by

Series title, number and report code of publication

VTT Publications 583
VTT–PUBS–583

Author(s)
Turunen, Erja

Title

Diagnostic tools for HVOF process optimization

Abstract

In the thermal spray process the coating is built up from lamellas formed by rapid solidification of the melted or semi-melted droplets attached to the substrate. A typical structure for the coating is a pancake-like lamellar structure, where the flattening stage and adhesion between the lamellas, together with the coating material itself, define the main properties of the coating. Thermal spray coatings are often applied for better corrosion and wear resistance. Therefore, low porosity and good adhesion are desired properties for the coating. High velocity processes – especially HVOF (High velocity oxy-fuel) spraying – are the most potential methods for producing a good adherent coating with low porosity.

From a scientific point of view, particle velocity and particle temperature, together with substrate temperature, are the main parameters affecting the deposit formation. They determine the deposit build-up process and deposit properties. Particle velocity and temperature affect the deposit efficiency as well as the microstructure.

The aim of this work was to show the workability of diagnostic tools in the HVOF process. The focus was on first order process mapping, including on-line diagnostics and single splat studies. Nanocrystalline alumina composites and quasicrystals were selected, two materials that are complex to spray. With both materials the melting state of the particles must be well optimized in order to produce dense, well-adhered coating without unwanted changes in coating phase structure.

The main focus was on the HVOF spraying of alumina. The target was to obtain a systematic understanding of the influence of the process conditions on the microstructure development in HVOF alumina coatings. Conventional limits of gas ratios and flows were exceeded to obtain a wide velocity-temperature range. The study aimed to produce information for a first order process map, and was carried out at a much deeper level than previously reported. Propylene and hydrogen as fuel gases were compared, and other variables, such as total gas flow rate, fuel gas/oxygen ratio, and standoff distance were also varied. The obtained data was applied for nanostructured alumina composite coatings, and the effect of the process conditions was compared on the obtained coating microstructure and properties.

On-line diagnostic measurements, in which particle temperatures and velocities in the flame can be measured, were performed. The main work was carried out for alumina by using a DPV-2000 system. Two clear regions of different temperature and velocity arise from the use of different fuel gases. Single splat studies correlated well with the obtained coating properties, and a first order process map for alumina was created showing the window for the spray parameters producing best coating quality plotted against coating hardness and abrasive wear resistance.

It was shown that diagnostic results can be correlated with the coating microstructure and coating properties in HVOF spraying. It was also demonstrated that the coating properties and coating quality can be improved by optimizing and carefully selecting the spray parameters.

Keywords

thermal spraying, HVOF, high velocity oxi-fuels, process optimizatic diagnostics, single splat studies, surface coatings, alumina, quasicrystals, nanofractions

Activity unit

VTT Industrial Systems, Metallimiehenkuja 8, P.O.Box 1703, FI–02044 VTT, Finland

ISBN			Project number
951–38–6677–7 (soft back ed.) 951–38–6678–5 (URL:http://www.inf.vtt.fi/pdf/)			
Date November 2005	Language English	Pages 66 p. + app. 92 p.	Price
Name of project		Commissioned by	
Series title and ISSN VTT Publications 1235–0621 (soft back ed.) 1455–0849 (URL: http://www.vtt.fi/inf/pdf/)		Sold by VTT Information Service P.O.Box 2000, FI–02044 VTT, Finland Phone internat. +358 20 722 4404 Fax +358 20 722 4374	

In the thermal spray process the coating is built up from lamellas formed by rapid solidification of the melted or semimelted droplets attached to the substrate. A typical structure for the coating is a pancake-like lamellar structure, where the flattening stage and adhesion between the lamellas, together with the coating material itself, define the main properties of the coating. High velocity processes especially HVOF (High velocity oxy-fuel) spraying are the most potential methods for producing a good adherent coating with low porosity.

From a scientific point of view, particle velocity and particle temperature, together with substrate temperature, are the main parameters affecting the deposit formation. They determine the deposit build-up process and deposit properties.

The aim of this work was to show the workability of diagnostic tools in the HVOF process. The focus was on first order process mapping, including on-line diagnostics and single splat studies. The main focus was on the HVOF spraying of alumina. The target was to obtain a systematic understanding of the influence of the process conditions on the microstructure development in HVOF alumina coatings. The study aimed to produce information for a first order process map, and was carried out at a much deeper level than previously reported. The obtained data was applied for nanostructured alumina composite coatings, and the effect of the process conditions was compared on the obtained coating microstructure and properties. Also quasicrystalline materials were studied by using same methods.

It was shown that diagnostic results can be correlated with the coating microstructure and coating properties in HVOF spraying. It was also demonstrated that the coating properties and coating quality can be improved by optimizing and carefully selecting the spray parameters.

Tätä julkaisua myy

VTT TIETOPALVELU
PL 2000
02044 VTT
Puh. 020 722 4404
Faksi 020 722 4374

Denna publikation säljs av

VTT INFORMATIONSTJÄNST
PB 2000
02044 VTT
Tel. 020 722 4404
Fax 020 722 4374

This publication is available from

VTT INFORMATION SERVICE
P.O.Box 2000
FI–02044 VTT, Finland
Phone internat. +358 20 722 4404
Fax +358 20 722 4374

ISBN 951-38-6677-7 (soft back ed.)
ISSN 1235-0621 (soft back ed.)

ISBN 951-38-6678-5 (URL: http://www.vtt.fi/inf/pdf/)
ISSN 1455-0849 (URL: http://www.vtt.fi/inf/pdf/)

Erja Turunen